

University of Windsor

Scholarship at UWindor

Electronic Theses and Dissertations

Theses, Dissertations, and Major Papers

2010

Power Management Methodologies for Fuel Cell-Battery Hybrid Vehicles

Ahmad Fadel
University of Windsor

Follow this and additional works at: <https://scholar.uwindsor.ca/etd>

Recommended Citation

Fadel, Ahmad, "Power Management Methodologies for Fuel Cell-Battery Hybrid Vehicles" (2010).
Electronic Theses and Dissertations. 8235.
<https://scholar.uwindsor.ca/etd/8235>

This online database contains the full-text of PhD dissertations and Masters' theses of University of Windsor students from 1954 forward. These documents are made available for personal study and research purposes only, in accordance with the Canadian Copyright Act and the Creative Commons license—CC BY-NC-ND (Attribution, Non-Commercial, No Derivative Works). Under this license, works must always be attributed to the copyright holder (original author), cannot be used for any commercial purposes, and may not be altered. Any other use would require the permission of the copyright holder. Students may inquire about withdrawing their dissertation and/or thesis from this database. For additional inquiries, please contact the repository administrator via email (scholarship@uwindsor.ca) or by telephone at 519-253-3000ext. 3208.

Power Management Methodologies for Fuel Cell-Battery Hybrid Vehicles

by

Ahmad Fadel

A thesis submitted to the Faculty of Graduate studies through Mechanical Engineering in partial fulfillment of the Requirements for the degree of Master of Applied Science at the
University of Windsor

Windsor, Ontario, Canada

2010

© 2010 Ahmad Fadel



Library and Archives
Canada

Published Heritage
Branch

395 Wellington Street
Ottawa ON K1A 0N4
Canada

Bibliothèque et
Archives Canada

Direction du
Patrimoine de l'édition

395, rue Wellington
Ottawa ON K1A 0N4
Canada

Your file Votre référence

ISBN: 978-0-494-88920-6

Our file Notre référence

ISBN: 978-0-494-88920-6

NOTICE:

The author has granted a non-exclusive license allowing Library and Archives Canada to reproduce, publish, archive, preserve, conserve, communicate to the public by telecommunication or on the Internet, loan, distribute and sell theses worldwide, for commercial or non-commercial purposes, in microform, paper, electronic and/or any other formats.

The author retains copyright ownership and moral rights in this thesis. Neither the thesis nor substantial extracts from it may be printed or otherwise reproduced without the author's permission.

AVIS:

L'auteur a accordé une licence non exclusive permettant à la Bibliothèque et Archives Canada de reproduire, publier, archiver, sauvegarder, conserver, transmettre au public par télécommunication ou par l'Internet, prêter, distribuer et vendre des thèses partout dans le monde, à des fins commerciales ou autres, sur support microforme, papier, électronique et/ou autres formats.

L'auteur conserve la propriété du droit d'auteur et des droits moraux qui protègent cette thèse. Ni la thèse ni des extraits substantiels de celle-ci ne doivent être imprimés ou autrement reproduits sans son autorisation.

In compliance with the Canadian Privacy Act some supporting forms may have been removed from this thesis.

While these forms may be included in the document page count, their removal does not represent any loss of content from the thesis.

Conformément à la loi canadienne sur la protection de la vie privée, quelques formulaires secondaires ont été enlevés de cette thèse.

Bien que ces formulaires aient inclus dans la pagination, il n'y aura aucun contenu manquant.

Canada

AUTHOR'S DECLARATION OF ORIGINALITY

I hereby certify that I am the sole author of this thesis and that no part of this thesis has been published or submitted for publication.

I certify that, to the best of my knowledge, my thesis does not infringe upon anyone's copyright nor violate any proprietary rights and that any ideas, techniques, quotations, or any other material from the work of other people included in my thesis, published or otherwise, are fully acknowledged in accordance with the standard referencing practices. Furthermore, to the extent that I have included copyrighted material that surpasses the bounds of fair dealing within the meaning of the Canada Copyright Act, I certify that I have obtained a written permission from the copyright owner(s) to include such material(s) in my thesis and have included copies of such copyright clearances to my appendix.

I declare that this is a true copy of my thesis, including any final revisions, as approved by my thesis committee and the Graduate Studies office, and that this thesis has not been submitted for a higher degree to any other University or Institution.

ABSTRACT

The implementation of fuel cell vehicles requires a supervisory control strategy that manages the power distribution between the fuel cell and the energy storage device. Some of the current problems with power management strategies are: fuel efficiency optimization methods require prior knowledge of the driving cycle before they can be implemented, the impact on the fuel cell and battery life cycle are not considered and finally, there are no standardized measures to evaluate the performance of different control methods. In addition to that, the performances of different control methods for power management have not been directly compared using the same mathematical models. The proposed work will present a different optimization approach that uses fuel mass flow rate instead of fuel mass consumption as the cost function and thus, it can be done instantaneously and does not require knowledge of the driving cycle ahead of time.

DEDICATION

To my parents, my teachers and anyone who ever shared their knowledge with me.

ACKNOWLEDGEMENTS

In the name of Allah, the Most Gracious and the Most Merciful

All praises to Allah for the strengths and blessings in completing this thesis. While the master's thesis project is an independent project, I believe what made my time as a master's student a great learning experience, are the people that I had the chance to work with. It all starts with my supervisor Dr. Biao Zhou, whose knowledge and support were very critical in helping me finish my project. My research colleagues were an integral part of my master's experience, their feedback and comments on my research work during our weekly meetings were all very helpful and allowed me to improve many aspects of my project. I would like to dedicate special thanks to Mr. Dan Dennome, Mr. Charbel Boutros, Mr. Yan Zhang, Mr. Anh Le Dinh, Mr. Srikanth Jonnalagedda and Ms. Xiaojing Liu.

The experimental part of the project was the most challenging and without the help of the Mechanical Engineering Department technicians: Mr. Andy Jenner and Mr. Patrick Seguin, it would not have been possible to finish the project smoothly. I would like to thank them for their help, and most importantly valuable technical feedback comments on my project designs.

I would also like to thank my parents Luay and Ahoud and my brother Osama for their love, support and encouragement. They are the reason behind my strive for success and courage to always keep trying.

TABLE OF CONTENTS

AUTHOR'S DECLARATION OF ORIGINALITY.....	III
ABSTRACT	IV
DEDICATION	V
ACKNOWLEDGEMENTS	VI
TABLE OF CONTENTS.....	VII
LIST OF FIGURES	IX
LIST OF SYMBOLS	XI
CHAPTER I. INTRODUCTION	1
1.1 STATUS OF ELECTRIC VEHICLES (FUEL CELLS VERSUS BATTERIES)	1
1.2 CHALLENGES FACING FUEL CELL VEHICLES	4
1.3 HYBRID FUEL CELL VEHICLE.....	5
1.4 ENERGY STORAGE DEVICE.....	6
1.5 POWER AND ENERGY MANAGEMENT.....	10
1.6 DIRECTION OF PRESENT RESEARCH.....	12
CHAPTER II. LITERATURE REVIEW	13
2.1 CONTROL METHODOLOGY	13
2.2 THESIS OUTLINE	18
CHAPTER III. CONTROL DESIGN	20
3.1 MATHEMATICAL MODELS.....	20
3.2 CONTROLLER DESIGN.....	30
3.3 PERFORMANCE MEASURES	40
CHAPTER IV. SIMULATION RESULTS.....	45
4.1 POWER DEMAND	45
4.2 BATTERY SOC VARIATION	46
4.3 FUEL CONSUMPTION	48
4.4 PARTIAL SOC BATTERY CYCLING	50
CHAPTER V. EXPERIMENTAL.....	53
5.1 EXPERIMENTAL SETUP	53
5.2 EXPERIMENTAL RESULTS.....	57
CHAPTER VI. CONCLUSIONS AND RECOMMENDATIONS	63

6.1 CONCLUSIONS.....	63
6.2 RECOMMENDATIONS.....	64
REFERENCES.....	67
VITA AUCTORIS.....	71

LIST OF FIGURES

Figure 1: Comparison of battery useful specific energy (Data taken from [3]).....	2
Figure 2: Comparing FCEV cost with the conventional ICEV (Data taken from [4]).....	3
Figure 3: Fuel cell vehicle powertrain	6
Figure 4: Battery electrochemistry.....	9
Figure 5: a) Plug-in hybrid configuration b) Non-plug-in hybrid configuration	10
Figure 6: Vehicle configuration	20
Figure 7: Fuel cell model	22
Figure 8: Fuel cell polarization curve	23
Figure 9: DC/DC voltage converter circuit.....	25
Figure 10: Battery equivalent circuit model	27
Figure 11: AC Motor characteristics.....	30
Figure 12: Motor efficiency map	30
Figure 13: Modes of operation: a) hybrid drive b) regen/charge sustaining.....	31
Figure 14: Pedal position	32
Figure 15: PID Controller diagram.....	33
Figure 16: Fuzzy logic controller.....	34
Figure 17: Acceleration efficiency test cases.....	35
Figure 18: Output membership functions	35
Figure 19: Input membership function	36
Figure 20: Surface plot of the fuzzy logic controller output.....	36
Figure 21: Fuel flow rate optimization surface plot.....	38
Figure 22: Optimization approach flow chart.....	39
Figure 23: SOC - Battery only simulation	43
Figure 24: Discharge cycle count - Battery only simulation	44
Figure 25: Simulation driving cycle	45
Figure 26: Simulation results: power demand	46
Figure 27: Battery SOC	47
Figure 28: Fuel consumption	49
Figure 29: System efficiency	50
Figure 30: Battery cycle count.....	51

Figure 31: Test bench schematic diagram 53
Figure 32: Flywheel kinetic energy 55
Figure 33: SAE Baja vehicle driving loads..... 56
Figure 34: Accelerated driving cycle..... 57
Figure 35: Total power demand comparison 58
Figure 36: Speed comparison..... 59
Figure 37: Experimental SOC variation 60
Figure 38: Experimental fuel consumption..... 61
Figure 39: Experimental battery cycle count..... 62
Figure 40: Option #1 for improving the test bench..... 65
Figure 41: Option #2 for improving the test bench..... 65

List of Symbols

V_{oc}	Fuel cell open circuit voltage (volts)
V_T	Fuel cell open circuit voltage as a function of temperature (volts)
V_{act}	Activation voltage loss (volts)
i_0	Exchange current density (Amperes)
V_{conc}	Concentration voltage loss (Volts)
P_{H_2}	Hydrogen gas partial pressure (atm)
P_{O_2}	Oxygen gas partial pressure (atm)
\dot{m}_{H_2}	Hydrogen gas mass flow (kg/s)
\dot{m}_{O_2}	Oxygen gas mass flow (kg/s)
U_{H_2}	Rate of utilization of hydrogen gas ($0 \leq U_{H_2} \leq 1$)
U_{O_2}	Rate of utilization of oxygen gas ($0 \leq U_{O_2} \leq 1$)
$\Delta \bar{g}_f$	Molar Gibbs free energy of formation at $25^0 C = -237,000$ J/mole
F	Faraday constant = 96485 C/mole
Δs	Change in entropy for the chemical reaction = -44.43 J/(mol. k)
T	Fuel cell operating temperature (K)
T_0	Standard room temperature (K)
R	Universal gas constant = 8.3144 J/ Kmol
α	Charge transfer coefficient = 0.5
i_{fc}	Fuel cell current (Amps)
A_{fc}	Fuel cell active area (m^2)
P_{fuel}	Absolute supply pressure of fuel (atm)
P_{Air}	Absolute supply pressure of air (atm)
$x\%$	Purity of fuel supply
$y\%$	Purity of air supply
N	Number of cells
M_{H_2}	Molar mass of hydrogen gas = 2.0158 g/mole
M_{O_2}	Molar mass of oxygen gas = 32 g/mole
V_{Out}	Output voltage of the DC/DC converter (Volts)
V_{FC}	Fuel cell voltage (Volts)

V_c	Voltage across the capacitor (Volts)
i_L	Inductor current (Amps)
D	Transistor switch duty ratio ($0 < D < 1$)
i_{out}	Output current of the DC/DC converter (Volts)
L	Inductance (H)
C	Capacitance (F)
V_{Batt}	Battery net voltage (Volts)
V_{Batt_OC}	Battery open circuit voltage (Volts)
I	Battery current (Amps)
R_i	Internal resistance (Ohms)
SOC	State of charge of the battery
Q	Rated battery capacity (Amp hour)
F_{Total}	Total traction force (N)
$F_{Rolling}$	Rolling resistance force (N)
F_{Drag}	Aerodynamic drag resistance force (N)
$F_{Gradient}$	Resistance force due to road gradient (N)
$F_{acceleration}$	Force required to accelerate the vehicle (N)
θ	Road gradient angle (degrees)
g	Gravitational constant (m/s^2)
Eff_{FC}	Instantaneous fuel cell efficiency
Eff_{Batt}	Instantaneous battery efficiency
Eff_{Hybrid}	Instantaneous system efficiency in the case of hybrid drive mode
Eff_{Regen}	Instantaneous system efficiency in the case of regenerative braking mode
Eff_{Charge}	Instantaneous system efficiency in the case of battery charging mode
HHV_{H2}	Higher heating value of hydrogen = 141.9 MJ/Kg
Eff_{DC}	Instantaneous DC/DC converter efficiency
P_{drive}	Power required by the electrical drive (watts)
$m_{fuel\ consumed}$	Hydrogen fuel consumed by the fuel cell (kg)

$\Delta E_{\text{recharge}}$	Change in energy due to change in state of charge of battery (Joules)
m_{recharge}	Hydrogen fuel required to charge the battery back to its initial state of charge (kg)
\dot{m}_{eq}	Equivalent mass flow rate (kg/s)
\dot{m}_{batt}	Equivalent mass flow rate of the battery (kg/s)
\dot{m}_{fc}	Fuel cell mass flow rate (kg/s)
SOC_{max}	Maximum allowed battery SOC = 80 %
SOC_{min}	Minimum allowed battery SOC = 40 %
c	A variable parameter that ranges from 0 – 2 depending on the battery SOC

CHAPTER I. INTRODUCTION

1.1 Status of Electric Vehicles (Fuel Cells versus Batteries)

With the growing demand for more efficient and more environmentally friendly automobiles, electric vehicles have come out as the most likely future of the automotive industry. The two main types of electric vehicles currently considered are battery and fuel cell powered vehicles. In the past two decades fuel cell and battery powered vehicles have received unprecedented increase in research funding, and nowadays almost every major automotive manufacturer has a prototype for a battery electric vehicle (BEV) or a fuel cell electric vehicle (FCEV). A good comprehensive review of the recently developed prototype vehicles is presented in [1]. Table 1 shows a summary of the most recent FCEVs. Even with the great efforts put in the research and development of fuel cell technology, none of these prototypes are being mass produced at the moment. The closest an FCEV has come to mass production is Honda's FCX Clarity [2], where a preproduction version of the vehicle was introduced in Japan and the United states in 2008. Currently, the FCX Clarity is only available in the Los Angeles area in North America, since it is one of the few places that have hydrogen refueling stations available.

Table 1: Current FCEV prototypes

Maker / Model	Year	Fuel Cell Size	Range	Equivalent MPG	Max Speed
Daimler / B-Class	2009	90 kW	616 km	90 mpge	170 km/h
Ford / HySeries	2007	85 kW	491 km	80 mpge	137 km/h
GM / Provoq	2008	88 kW	483 km	60 mpge	160 km/h
Honda / FCX	2007	100 kW	570 km	70 mpge	160 km/h
Toyota / FCHV	2008	90 kW	830 km	68 mpge	155 km/h

Despite the fact that during the past two decades, the automotive industry has focused its efforts on FCEVs, today with the increased popularity of hybrid electric vehicles (HEV), plug-in hybrid electric vehicles (PHEV) and pure electric vehicles powered by batteries (BEV) has forced FCEVs to be put on the backburner of the automotive industry's research efforts. This is mainly due to the great improvement in battery technology, which has changed researchers' efforts to focus on battery based vehicles.

While both fuel cells and batteries generate electricity to drive electric motors, fuel cells derive their energy from hydrogen stored onboard the vehicle, batteries on the other hand, obtain their energy from the electrical grid or stationary generators. Both have their advantages and disadvantages, however, a study done by Thomas at H₂Gen Innovations Inc [3] shows “the advantages of the fuel cell vehicle are dominant if the battery vehicle must have 480 km range to serve as a fully functional all-purpose passenger vehicle”. The work comparison by Thomas covers three main criteria: vehicle mass, greenhouse gases emission and vehicle cost. In terms of vehicle mass, Figure 1 shows how the specific energy (Wh/kg) of various battery types compare with the specific energy that can be obtained from a 35 MPa and 70 MPa hydrogen tank. It is clear to see that a 35 MPa hydrogen tank can provide the same amount of energy with half the weight required for a lithium-ion battery stack. This difference in energy density can prove to be a big factor, since as the required electric vehicle range increases, the weight of the vehicle will have to increase significantly to account of the additional battery units, which in turn reduces the vehicle equivalent fuel efficiency.

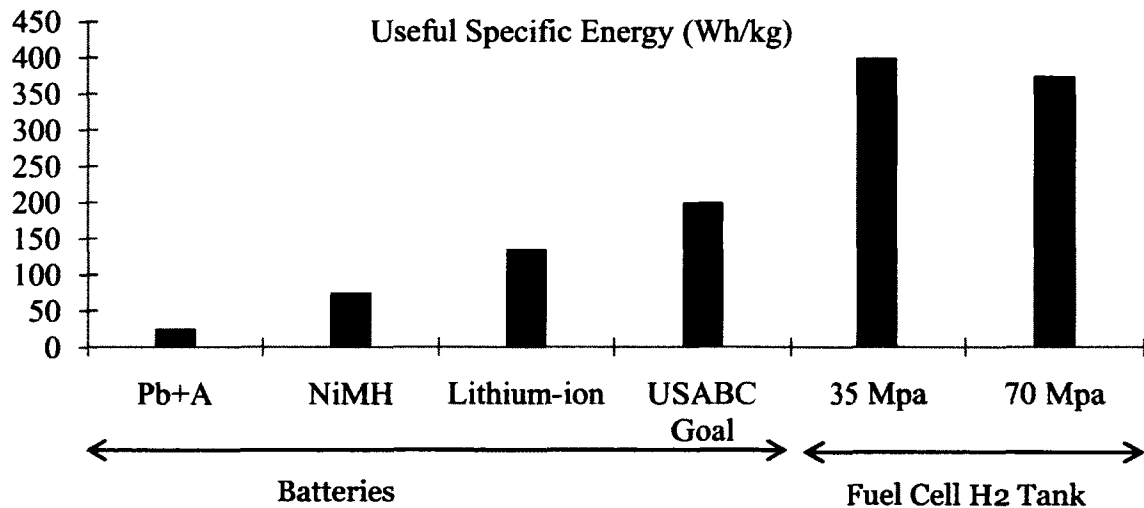


Figure 1: Comparison of battery useful specific energy (Data taken from [3])

In terms of the greenhouse gas emissions, the main concern is how does the environmental impact resulted from generating hydrogen required for fuel cell engines compares to the impact of the extra needed electricity generation to charge the batteries in electric vehicles. Currently, in North America almost 50 % of the electricity generated

comes from coal, and the average electrical grid efficiency is only 35 %. Hydrogen on the other hand is produced using the steam reforming process which depends on fossil fuels such as natural gas or coal with 80 % efficiency.

In terms of vehicle cost, the work done by Kromer and Heywood [4] presents a comprehensive comparison of mass production costs for different alternative energy vehicles with respect to conventional internal combustion engine vehicles. Their work shows that the production cost for battery powered electric vehicles mainly depends on the range the vehicle is expected to cover before having to recharge its batteries, as the required range increases the cost significantly increases. For a battery electric vehicle with 320 km range the mass production cost would be approximately \$10,200 more than conventional vehicles, while if mass produced a fuel cell electric vehicle with a 560 km range would cost approximately \$3600 more than conventional vehicles. Figure 2 shows how the fuel cell vehicle mass production cost compares with hybrid electric, plug-in hybrid electric and battery vehicles.

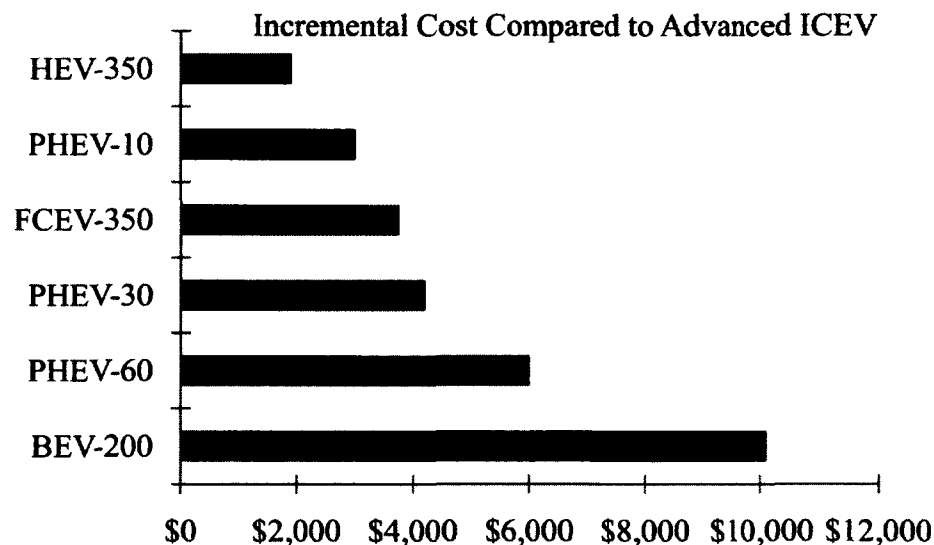


Figure 2: Comparing FCEV cost with the conventional ICEV (Data taken from [4])

Essentially, the comparisons presented show that unless a significant breakthrough in battery technology that enables batteries to achieve higher energy densities, battery powered, hybrid electric and plug-in hybrid electric vehicles will

continue to be the short term solution in the automotive industry. While BEV might be more superior for applications that do not require long range, FCEV is still the solution that will provide an all around vehicle.

1.2 Challenges Facing Fuel Cell Vehicles

Polymer Electrolyte Membrane Fuel Cells (PEMFCs) have received particular attention for vehicle applications because of their smaller size, lower operating temperature and relatively rapid start-up time. The simplest and most practical PEMFC systems for powering a car are those where the fuel is converted directly to electricity, for example: direct-hydrogen or direct-methanol PEMFCs [5]. There are various challenges that face the implementation of fuel cell vehicles, the most obvious of these challenges are: lack of hydrogen fuel infrastructure and the safety of hydrogen fuel storage on board of the vehicle. However, an important challenge that must not be overlooked is the overall efficiency and stability of the fuel cell. In order for fuel cells to challenge internal combustion engines in automotive applications, they must achieve higher overall power efficiency. One of the key areas where internal combustion engines excel is their ability to accommodate transient load demands such as acceleration or hill climbing with a fairly constant efficiency range. Fuel cells on the other hand, have a much slower response time due to the fact that, the fuel cell engine itself is comprised of other smaller subsystems such as: Air compressor, humidifier, flow regulators and pressure valves, and thus the fuel cell engine can only respond to high transient load demands as fast as its subsystems response. In addition to that, the fuel cell response time is limited by the rate of reaction that takes place at the membrane assembly and is also affected by the water and thermal management within the membrane. In their analysis of the fuel cell dynamic response, Choa et al [6] simulates the transient power requirement by the driver in acceleration, deceleration and start-up. Using experimental data, they show that the fuel cell response exhibits a delay time and “undershoot/overshoot” when exposed to varying operating conditions, furthermore, they go on to relate the response time to the air supply, fuel supply and the water content in the fuel cell. Another problem with fuel cells is durability. It has been shown in literature [7]; even if the fuel cell is able to keep up with the transient power demand required by the vehicle, the constant power cycling and stop-

go nature of automobiles will significantly reduce the fuel cell lifetime and performance. Adding to the difficulties is the fact that fuel cell systems are becoming more complex due to the addition of subsystems such as heat exchangers and humidifiers to maintain optimal operating conditions.

1.3 Hybrid Fuel Cell Vehicle

Due to the reasons mentioned previously, fuel cells are not used to support the vehicle power demand alone, but instead, they are coupled with an energy storage device in order to accommodate the transient power demand and improve efficiency. This concept can also be referred to as the hybrid fuel cell vehicle, where the hybridization is between an energy conversion engine and an energy storage device. The inclusion of the energy storage device (such as a battery) might seem to go against the goal of concentrating on the fuel cell powered vehicle as apposed to the battery powered vehicle, however, the size and use of the energy storage device will be very much limited to the bare minimum to recuperate regenerative braking energy and help the fuel cell in fast transient power demand situations.

The main components of this powertrain layout are: the air supply system which controls the rate at which air is supplied to the cathode side of the fuel cell, the hydrogen supply system which controls the rate of hydrogen supply, the energy storage device that supplies transient power and recovers regenerative braking energy, the electric drive which propels the vehicle base on the road loads applied to the wheels and power conditioning components such as DC/DC Converters, which are used to boost the fuel cell voltage to the required electric drive voltage. Also a power management unit is needed to control the power flow from the fuel cell and from/to the energy storage device. Most of these components are not mechanically coupled and thus a control algorithm that uses sensors and actuators must be implemented to monitor the operation status of the system and manage the power demand between the fuel cell and the energy storage device. Therefore, control design is a critical factor that can have a great impact on the overall efficiency of the system. The main role of the controller is to take the driver command (throttle position) and based on that adjust the operation of the fuel cell

powertrain components. Since each component has its own control variables and must be adjusted individually, a supervisory control algorithm is used to send control signals to each one of the powertrain components such as the air supply, hydrogen supply, and the power management unit. This supervisory controller is therefore analogous to the engine control unit (ECU) in an internal combustion engine vehicle. A layout of the fuel cell-battery hybrid powertrain is shown in Figure 3.

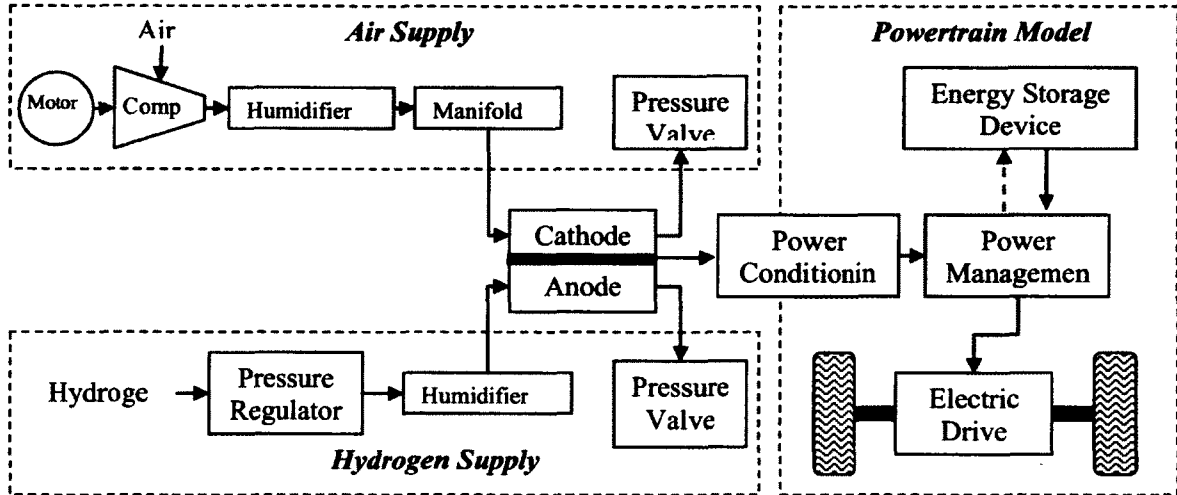


Figure 3: Fuel cell vehicle powertrain

1.4 Energy Storage Device

There are two main types of energy storage devices that can be coupled with the fuel cell to accommodate the transient power demands, these devices are: batteries and ultracapacitors. Batteries generally have higher energy density than ultracapacitors (batteries: $20\text{-}80 \text{ Whkg}^{-1}$, and ultracapacitors: 15 Whkg^{-1}), while ultracapacitors feature high power density [8]. Choosing the appropriate energy storage device type is dependent on the application; ultracapacitors for example are more suitable for applications with high transient loads under short periods of time, while batteries are suitable for applications where higher loads are required for longer periods of time. For the purpose of building an all around vehicle that is capable of handling both highway and city driving conditions, a battery stack was selected as the energy storage device.

The battery technology implemented in electric and hybrid electric vehicles covers the following types of batteries: lead acid batteries, nickel-based batteries (nickel/cadmium and nickel-metal hydride) and also lithium-based batteries, either lithium-ion or lithium-polymer batteries. While very economical and widely used, the lead acid battery has proven its shortcomings when applied in electric vehicles, due to its low voltage potential and large size for high voltage applications. Nickel-metal hydride have been initially considered as the front runners for the electric and hybrid electric vehicle problem, however, their significant capacity degradation during deep cycling and memory effects in short cycling has made them not a viable solution for automotive applications. Lithium-based batteries on the other hand, have been widely used in portable electronics applications such as laptops and cell phones. Due to the high voltage potential and the light weight offered by lithium-based battery chemistries, they are currently considered the future solution that will make electric vehicles an affordable and sustainable solution. However, due to their high sensitivity to being overcharged, over discharged or abnormal thermal conditions in the surroundings, there is a big safety concern associated with lithium-based batteries and in fact they can not be implemented without the use of an electrical and thermal battery management system, which complicates the implementation of these batteries. Nonetheless, lithium-based batteries are still considered future of the automotive industry and ongoing research efforts are continually improving lithium chemistries to make them more viable for automotive applications.

Lithium-based batteries are classified into two types: lithium-polymer and lithium-ion based. While lithium-polymer batteries have shown great potential with their ability to be formed in different geometrical shapes, they are ever more sensitive to temperature and charge limits, thus they present even more safety concerns. Lithium-ion type batteries are divided based on the cathode material, with the most popular being cobalt based, manganese based and lithium iron phosphate cathodes. A comparison between the voltage potential obtained from each type cathode is shown in Table 2. The comparison first shows the significant difference in voltage potential between lead acid and nickel-metal hydride and lithium based batteries. Also shown is how different

cathode materials impact the voltage potential, where manganese based cathodes result in the highest potential of 4.0 volts. The cathode material selected for the battery stack considered in this study is Lithium iron phosphate (LiFePO₄). While LiFePO₄ has a relatively lower potential voltage, it also shows higher energy density, which means lighter weight in automotive applications. In addition to that, it is currently the least expensive of any of the different lithium-based batteries.

Table 2: Different battery chemistries comparison

Type	Cell Voltage	Energy Density
Lead Acid	2.1 V	0.14 MJ/kg
Nickel-Metal Hydride	1.2 V	0.36 MJ/kg
LiFePO ₄	3.3 V	0.495 MJ/kg
LiMn ₂ O ₄	4.0 V	0.400 MJ/kg
LiCoO ₂	3.7 V	0.518 MJ/kg

1.4.1 Battery Degradation

One of the main problems with hybrid powertrain configurations is the cycle life of the energy sources. In the case of hybrid configurations where fuel cells are the energy conversion devices, power management is normally designed to favor longer lifespan for the fuel cell engine by limiting its transient response and also the magnitude of its response. The lifespan of the battery on the other hand is mainly considered by designing power management strategies that will either sustain the state of charge of the battery at a certain level or prevent deep discharge cycles. The battery however is still subjected to an extensive amount of charge/discharge cycles, which will have a great impact on its cycle life, even if those cycles are partial cycles and not deep discharges. In order to examine the impact of these cycles on the battery life, it is first very critical to look at the principle of battery electrochemistry. A schematic to illustrate the operation of a lithium based battery is shown in Figure 4. The chemical reactions that take place are divided into the anode half and the cathode half, for the case of cobalt-based cathode material, the chemical reactions become:

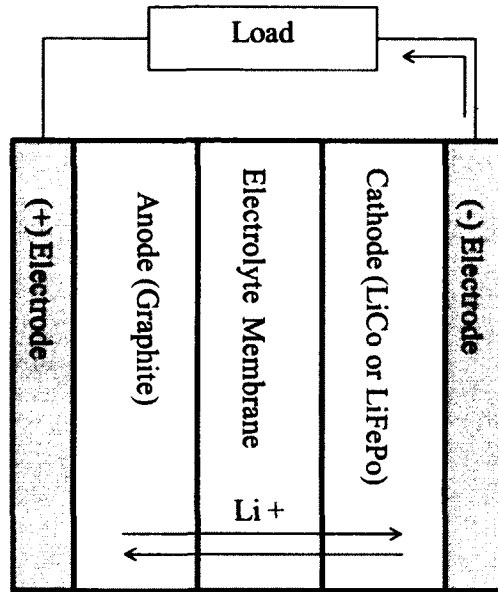
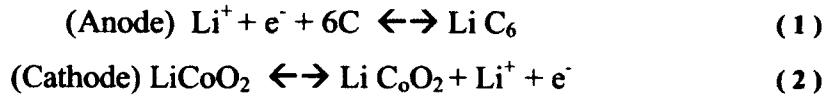


Figure 4: Battery electrochemistry

Essentially, the chemical reactions describe the removal of lithium ions from the anode and addition in the cathode. This process takes place when the battery is being discharged. In the case of charging the battery, the process is reversed and lithium ions are extracted from the cathode and inserted in the anode. Deep discharges of the battery will result in a very important phenomenon known as the formation of passivation layer SEI (Solid Electrolyte Interface) [9] on the surface of the anode. This passivation layer is mainly created in the first charging cycle of the battery and results in a significant loss of lithium that is normally cycled between the anode and the cathode.

Another phenomenon that takes place during deep discharge and charge cycling is the formation of a surface film on the anode side. This surface film however, has less to do with the battery cycle life loss than the increase in the battery internal resistance. The last main phenomenon that contributes to battery degradation is the loss of electrode active material particularly on the anode, which causes fracture of the graphite plane due

to excessive mechanical stresses and blocking of the intercalation site by undesired species intercalation

1.5 Power and Energy Management

Essentially, the implementation of a hybrid fuel cell powertrain configuration has two main purposes: Allow the vehicle to recapture braking energy by storing it in the battery stack and also allow the vehicle to handle any transient demands imposed by the road loads. In general there two main types of hybrid powertrain configurations: parallel or series. As the name might intuitively imply, in a series configuration the battery acts as a buffer between the fuel cell engine and the electric drive and thus the fuel cell's only function in this configuration is to maintain the state of charge of the battery. In the parallel configuration on the other hand, both the fuel cell and the battery stack are connected to the electric drive. Within a parallel or series configuration however, there is another dimension to the configuration, which is to have a plug-in or non-plug-in battery stack as shown in Figure 5.

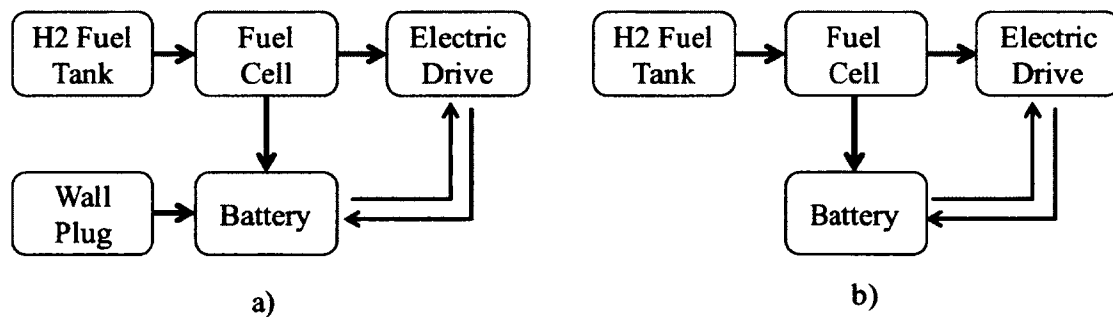


Figure 5: a) Plug-in hybrid configuration b) Non-plug-in hybrid configuration

The focus of the research presented in this thesis is hybrid fuel cell powertrains in a non-plug-in parallel configuration. Thus, this simplifies the energy management since the energy needed to drive the vehicle is strictly coming from the hydrogen fuel tank or recuperated energy stored in the battery through generative braking. From a total power demand point of view, the addition of a battery stack in parallel means the power needed to move the vehicle at any time instant can follow three options to the electric drive: 100 % from the fuel cell, 100% from the battery or a combination of both the fuel cell and battery. Which means choosing the appropriate distribution between the battery and the

fuel cell adds another dimension to the design process of such powertrains. The power between the fuel cell and the battery must be split in a way that gives the highest efficiency and prolongs the cycle life of the powertrain components. This can only be achieved with a power management strategy implemented at each time instant using a feedback controller.

In general, power management in hybrid powertrains can be classified into three main categories: load leveling, load following and rule based. A load leveling strategy would utilize the battery power for handling the quick transient power demands of the electric drive and thus allowing the fuel cell to operate in a more steady state conditions. A load following strategy splits the power demand between the fuel cell and the battery stack in a way that optimizes a predefined goal (be it fuel consumption or component health), thus with this strategy has two functions: to handle the transient demands and to also share the overall loads of the driving cycle with the fuel cell. The rule based type power management strategy is simply a combination both the load leveling and the load following strategies. It operates by establishing a set of control rules that manage the operation of the system components to either be load leveling or load following depending on the status of the fuel cell and the battery. Finding the most appropriate power management strategy will obviously vary depending on the application. However, it is critical to obtain a direct comparison between these power management strategies to see how each one impacts the overall vehicle performance and life time cycle.

Before designing such a power management strategy, it is critical to establish design goals. These goals can be either based on reducing the vehicle fuel consumption or improving the cycle life of the powertrain components. Thus, the design of the power management strategy becomes an optimization problem with a set of predefined goals. However, achieving both of these goals at the same time might present a dilemma in the design of power management strategies, since as the fuel consumption is reduced the impact on the fuel cell and battery cycle life might be too severe. Therefore, a compromise between optimizing the power management strategy for fuel consumption and prolonging the fuel cell and battery life is needed.

1.6 Direction of Present Research

Given the brief introduction, this research work will focus on the design and implementation of a power management strategy for a fuel cell-battery hybrid vehicle. In particular this research work will look into the implications of selecting different control methods for power management in hybrid powertrains. The main question investigated in this study is “how does the control method impact the performance of the power management strategy?”, where the performance will be defined in terms of efficiency, fuel consumption, and also battery cycle life. This question will be investigated by designing from scratch several controllers for power management for the same vehicle application. Performance measures will then be developed to directly compare the effectiveness of each control method. The investigation will be carried on by using both mathematical simulation and also experimental setup. The experimental setup serves as a prototype for a small fuel cell vehicle powertrain, and will to an acceptable degree of accuracy simulate the road loads experienced by a vehicle in city driving conditions. Using the experimental setup, it will be possible to monitor the current, voltage, speed and torque measurements of the system and thus, these variables can be used in a hardware-in-the-loop configuration to implement the designed power management controllers.

CHAPTER II. LITERATURE REVIEW

2.1 Control Methodology

A literature survey shows that various forms of control methods have already been considered and implemented for power management between the fuel cell engine and an energy storage device. These control methods can be summarized:

1. Classical PID control methods
2. Rule based control methods
3. Optimization control methods

The theory behind and the existing work done on each one of the above control methods will be explained in this section.

2.1.1 Classical PID control methods

One of the most commonly used control methods in literature are the PID classical control method. Jiang et al. [10] presented a PID controller for an active FCV configuration (i.e., the fuel cell is connected directly to the voltage bus). Thounthong et al. [11] on the other hand presented a PID controller for a passive FCV configuration (i.e. the fuel cell is not connected directly to the voltage bus). In both of the mentioned PID controllers, the battery state of charge and the battery current are used in feedback loops to generate the fuel cell current command. The ultimate goal in this control method is to monitor and maintain the state of charge of the (SOC) battery at its nominal value of 60 %, this is because as the battery is charged and discharged more frequently, its internal resistance increases over time resulting in increasing the voltage loss. Thus, maintaining a nominal SOC will extend the battery life and improve its performance. In the case where the SOC of the battery drops significantly below the reference value, a current request is sent to the fuel cell in order to charge the battery. The magnitude of fuel cell current request is also controlled by the power needed to drive the vehicle. In order to satisfy both the battery SOC and the vehicle power demand, two control loops are required; battery current control loop and a fuel cell current control loop. Therefore, the main variables that impact the control algorithm are: the measured battery SOC and the measured battery current. A PID controller is used to compare the calculated SOC with a reference value to generate a battery current demand signal. This generated signal is then

used as a reference value for the battery current. Another PID controller is then used to generate a fuel cell current demand based on the difference between the battery current and its reference value.

The main advantages of the PID control method for hybrid fuel cell vehicle powertrains are its simplicity and ease of implementation, and also the fact that PID controllers are easily tuned. In addition to that PID controllers are commonly used in a wide range of applications and are the most basic form of control and thus there are various methods and rules to designing PID controllers.

The downside of using this type of control method is the fact that the controller does not take into consideration the fuel consumption or the overall efficiency of the powertrain. The PID control method focuses two objectives, which are maintaining the SOC of the battery at a desired level and sharing the transient load of the vehicle between the battery and the fuel cell. While this might improve the battery and the fuel cell expected life cycle and enable the vehicle to take on any transient road loads, it does not take into account minimizing the fuel consumption and maximizing the efficiency of the powertrain. Also the PID control parameters might be designed initially for a certain driving cycle or several driving cycles, however, this does not guarantee that the control parameter selected will function as designed given a change in driving conditions that has not been considered when designing the control parameters. In other words, the PID control parameters must be variable to accommodate for all possible driving conditions or driver requirements.

2.1.2 Rule based control methods (fuzzy logic controllers)

While in some textbooks they are referred to as “heuristic controllers”, essentially the rule based control methods use a set of predetermined rules that dictate the powertrain behavior and the power distribution between the fuel cell and the energy storage device. A simple example of rule based controllers is presented in [12] for hybrid electric vehicle applications, where the power split is between an internal combustion engine and a battery stack. The first step is for the controller to determine the mode of operation of the

powertrain, generally speaking there two main modes: traction and regenerative braking. The mode can be determined by comparing the power command to drive the vehicle with the power needed to slow down the vehicle, if the power command is higher than the brake power then the mode of operation is traction; otherwise it is safe to assume that the vehicle is in regenerative braking mode. In the case when the vehicle is operating in traction mode, the power split is dependent on the SOC of the battery. If the SOC of the battery is below the specified threshold, then the engine is forced to supply power to both propel the vehicle and recharge the battery. If on the other hand, the SOC is higher than the threshold range, the power required to propel the vehicle is obtained entirely from the battery. In cases when the required power to propel the vehicle is above the engine's limit, both the battery and the engine combine to propel the vehicle. A similar rule set would be applied in the case of a fuel cell and any type of energy storage device.

There are two ways to implement the rule based controller, either using Boolean logic or fuzzy logic control. Both types of controllers are based on a set of "if-then" rules, where input variables are compared to the rules in order to determine the output variables. However, the main difference between Boolean logic and fuzzy logic is that Boolean logic assigns the input to either a true or false (a value of 1 or a value of 0), while fuzzy logic allows the input to a range of values between 0-1. Thus, the difference between the fuzzy and Boolean is in the transition from one extreme rule case to another, where fuzzy allows for a more smooth transition. In addition to that, fuzzy logic classifies the input and output variables into "membership functions" described linguistically with words such as "high" or "low", where the definition of these membership functions depends on the control designer. An example of a membership function could be the range of power demand to propel the vehicle, if the power demand is greater than zero kW and less than 1000 kW, then the input corresponds to the "Low" membership function and so on a power range could be defined for "medium" and/or "high" membership functions. The use of the membership functions allows the designer to classify the input and output variables as they would be perceived by a human operator, and thus the rules can be set based on the membership function as well.

The fuzzy logic control method can be used to implement a power management controller by using the command power required to propel the vehicle and the SOC of the energy storage device as inputs and the fuel cell current as the output of the controller. Implementation of this type of control can very well be found in recent literature publications for fuel cell electric vehicles. One of the earlier works on power management with a fuzzy logic based controller is presented by Jeong et al. [13], where the load sharing between a fuel cell and a battery stack is controlled by managing the state of charge and current of the battery. Different types and sizes of energy storage devices have also been used for fuel cell vehicles, Kisacikoglu et al. [14] presented a fuzzy logic controller for an ultracapacitor based FCEV. Gao et al. [15] on the other hand utilized a fuzzy logic based controller for a hybrid vehicle that used two types of energy storage devices; a battery and an ultracapacitor.

While fuzzy logic controllers might seem as a good solution for the power management controller problem, there lays a major obstacle in designing fuzzy logic controllers. The main difficulty with fuzzy logic controllers is how to determine the appropriate number of member functions or range of values for the input and out variables. In other words, fuzzy logic controllers require training data in order to correctly form the membership functions and set of “if - then” rules. In most of the studies presented previously, the membership functions and rules were formed based on the common sense knowledge of the designer about the behavior of the energy storage device and the fuel cell. While designing the fuzzy logic controller based on common knowledge of the sub systems might work, it does not guarantee the vehicle will achieve optimal operation. One way to overcome this problem is to run experimental tests to provide the training data needed, however, this might not be feasible, especially when the vehicle is still in the design process.

2.1.3 Optimization control methods

As previously stated, the main goals for the hybrid control strategy are maximizing the overall efficiency of the powertrain, minimizing the overall fuel consumption and also maintaining the state of charge of the energy storage device within

an acceptable range. If formulated mathematically, then these goals can be used as the constraints for a simple mathematical optimization problem. Essentially, the goal of the optimization would be to find the most fuel efficient power split between the two energy sources in a hybrid powertrain, while maintaining acceptable operating conditions. In [16], [17] and [18] it can be seen that this type of optimization has already been investigated for hybrid electric vehicles, where the two energy sources are an internal combustion engine and a battery stack. In this case the optimization problem can be defined as: for a given driving cycle find the control law (or power split parameter) that will optimize the overall fuel consumption of the vehicle over the entire drive cycle. From this definition, it is now possible to form a cost function:

$$J_f = \int_0^{t_{final}} \dot{m}_f dt \quad (3)$$

Where \dot{m}_f is the flow rate of the fuel consumed, and thus, the cost function J_f is the amount of fuel consumed over the driving cycle period from time $t=0$ to $t=t_{final}$. The other aspect of the optimization is the SOC of the battery stack, which can be accounted for as a constraint on the optimization problem:

$$SOC_{final} = SOC_{initial} \quad (4)$$

$$SOC_{min} < SOC_{initial} < SOC_{max} \quad (5)$$

Now that the optimization problem is formulated, solving it can be done using several well known mathematical optimization algorithms. A good example that is often used is Pontryagin's minimum principle [19].

The same principle can also be applied to fuel cell electric vehicles, however, since the energy storage device is to be strictly charged from the fuel cell (i.e. not plug-in) an equivalent fuel consumption in terms of the hydrogen fuel must be considered. Li et al [20] presents a detailed procedure on using the optimization control method for fuel cell electric vehicles. In his work Li uses a combination of fuzzy logic type controller along with an optimization scheme; where in this case the control variables to be determined are the fuzzy logic parameters. Thus, Li uses a fuel consumption cost

function in order to optimize the fuzzy logic controller parameters. Doing so solves the problem with fuzzy logic controllers mentioned previously, which is the uncertainty in selecting the appropriate membership function parameters.

In addition to being able to maximize the fuel efficiency of the powertrain, optimization techniques can also be used to size the vehicle components. For example the work done in [21] optimizes a fuel consumption cost function to determine the best ratio of fuel cell to battery size in a fuel cell electric vehicle powertrain. However, a big disadvantage with optimization methods is the need to know the driving cycle ahead of time in order to optimize the cost function, which makes it difficult to implement in real-time vehicle applications. Although some researchers [22] have proposed using the GPS (global positioning system) to predict the driving route that the driver intends on taking and thus, using this data to optimize the control strategy as the vehicle begins the trip. While it is an innovative way to optimize the controller, using the GPS might not always be feasible, not mentioning the added vehicle cost to install a reliable GPS unit. Thus, even with the optimization techniques, there is still a need to develop a real time controller that does not require knowing the drive cycle ahead of time. Nonetheless, even if the optimization method is not applicable in real-time, it can still be a good designing technique used to obtain reference data to develop real-time controllers, such as the work done in [20] to design the fuzzy logic controller parameters. It can also be used as a system component sizing technique during the designing process of hybrid vehicles.

2.2 Thesis Outline

The main focus of this work is the design of a hybrid fuel cell vehicle power management control strategy. In particular this work is focused on hybrid configurations where a battery stack is used as the energy storage device. As can be seen from the literature review, there have been various types of controllers designed for managing the power split between the fuel cell and the battery stack. However, the literature review also shows that there is still room for improvement in the power management control strategy, some of the obvious problems with the current control strategies can be summarized as follows:

- Fuel efficiency optimization methods require prior knowledge of the driving cycle before they can be implemented
- The impact on the fuel cell and battery life cycle are not considered when designing power management control strategies
- There is no standardized method to evaluate the performance of different control methods
- Lack of direct comparison of different control methods for the same vehicle application

Thus, based on these drawbacks of the current control strategies, the scope of work of this project can be outlined by the following steps:

- Step1.** Size the components of a fuel cell-battery hybrid vehicle powertrain
- Step2.** Develop mathematical models for each component of the hybrid vehicle powertrain
- Step3.** Design and implement an improved power management controller
- Step4.** Develop performance measures that can be used to evaluate the performance of different control methods
- Step5.** Validate the effectiveness of the controller experimentally

CHAPTER III. CONTROL DESIGN

3.1 Mathematical Models

The mathematical models for each one of the vehicle components are implemented in MATLAB/Simulink. The vehicle chosen as the application case for this study is the SAE Baja vehicle designed and built by undergraduate students at the University of Windsor [23]. The main advantages of using the SAE Baja vehicle is its availability for experimental testing, simplicity of powertrain components and also relative ease of mathematical modeling. The SAE Baja vehicle typically has a top speed of 50 km/h and acceleration of 0-30 km/h in 4 seconds. This type of vehicle is normally referred to as a “Low Speed Vehicle”, and is often used to complement primary vehicles in industrial and transportation applications, such as warehouses, factories and airports. Despite the fact that the SAE Baja vehicle does not fall under an actual road vehicle weight class, the conclusions obtained from this study can still be generalized and considered when designing control algorithms for fuel cell vehicles. The powertrain configuration for this study is shown in Figure 6.

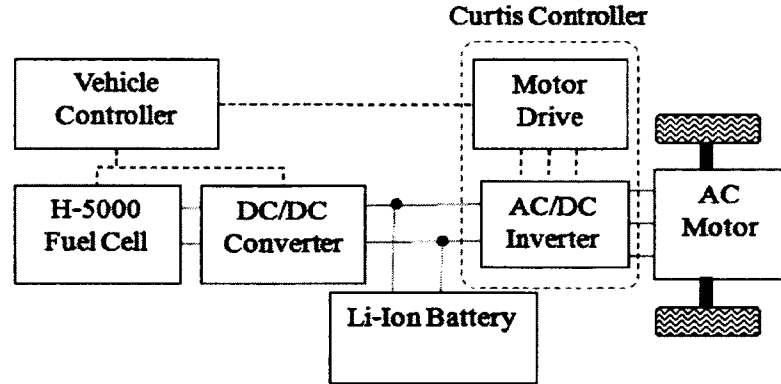


Figure 6: Vehicle configuration

Normally, the SAE Baja vehicle is equipped with a 10 Hp internal combustion engine, therefore, a 5kW fuel cell engine, a 10 Ah Lithium-ion battery stack and a 13 kW AC Induction motor were selected to propel the SAE Baja vehicle. Due to its higher efficiency, an AC induction motor was selected to drive the SAE Baja vehicle. The main parameter used to select the motor is the torque required to propel the vehicle. The selected AC motor has rated torque and speed of 100 Nm and 6000 rpm, which is

sufficient to propel the SAE Baja vehicle at a speed of 30 km/h and maximum road slope of 15 degrees. In order to control the AC motor and interface it to the DC bus, a vector drive controller/inverter combination that are normally used for electric fork lift utility vehicles was selected. The advantage of the selected motor controller/inverter is that it is capable of operating at a relatively low voltage. The motor controller/inverter is rated at 48 Volts and 350 Amps. The fuel cell selected for this application is the H-5000 manufactured by Horizon Fuel Cell Technologies [24], which has a rated power of 5kW, output voltage range of 64 V – 114 V and a system efficiency of 40% at 72 volts. The fuel cell does not incorporate a fuel reformer and thus the fuel is 99.99% pure hydrogen gas. A DC/DC converter is required to match the voltage of the fuel cell with the electric drive voltage (48 Volts). However, in this project the DC/DC converter and fuel cell will be simulated using a programmable power supply, thus, a DC/DC converter was not selected.

Lithium-ion batteries are classified in terms of the cathode material used to transfer ions from a typically graphite anode (LiC_6). The lithium ion battery selected for this project uses a lithium iron phosphate (LiFePO_4) cathode material. Lithium iron phosphate batteries have an average open circuit voltage of 3.3 Volts, although not as high as lithium ion polymer batteries (4.2 V), lithium iron phosphate cathode material is significantly less expensive. Thus, in order to match the voltage requirement for the electric drive, at least 15 lithium iron phosphate cells have to be connected in series to provide 48 volts. The capacity of the cells selected is 10 Ah, in order to obtain higher capacity more cells have to be connected in parallel, however, in this project 10 Ah is considered sufficient since the powertrain will be simulated over a maximum 30 minutes driving cycle. Choosing a low capacity also helps in illustrating the change in the SOC of the battery during the driving cycle simulation.

3.1.1 Fuel Cell Model

Obtaining a dynamic model that accurately describes all operating aspects of the fuel cell is a very challenging task. In order to obtain a complete fuel cell model, all the auxiliary devices such as the air compressor, the fuel (hydrogen) pump, heat exchangers

and flow regulators on each side the cathode and the anode must be considered. Despite, the fact that such model would give a great insight into the relationship between the fuel consumption, fuel cell operating conditions and the different energy management schemes, the model would be very nonlinear and would very much complicate the overall vehicle model. Alternately, for the purpose of developing a vehicle controller, the fuel cell model is simplified by modeling the fuel cell as a voltage source. Thus, the fuel cell model considered for this project is a simplified version that mainly takes into consideration the electrical and fuel flow rate behavior in the fuel cell. Figure 7 shows a schematic of the model.

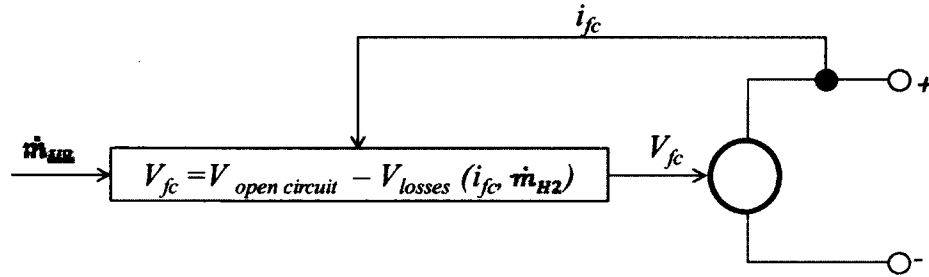
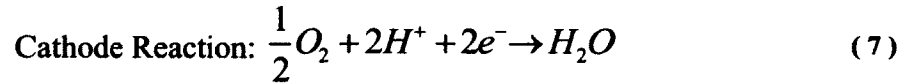
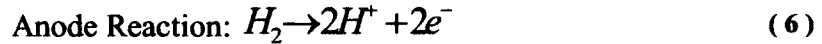


Figure 7: Fuel cell model

The reactions that take place at the fuel cell anode and cathode are:



From the anode side reaction it can be seen that for every molecule of water formed, there are two electrons passed through the load circuit. The energy required to form one mole of water is referred to as the Gibbs free energy of formation ($\Delta\bar{g}_f$). In order to find the reversible open circuit voltage, it is assumed that there are no losses and thus, all of the Gibbs free energy is converted to electrical power. The charge transferred for every mole of water formed can be determined using Faraday's constant (F) and so the reversible open circuit voltage (V_{oc}) is [25]:

$$V_{oc} = \frac{\Delta\bar{g}_f}{-2F} = \frac{-237,000 \text{ J/mole}}{\left(2 \frac{\text{mole e}}{\text{mole reactant}}\right) (96400 \text{ C/mole})} = 1.229 \text{ Volts} \quad (8)$$

It is important to note that the Gibbs free energy varies at different temperatures. Thus, the $\Delta\bar{g}_f$ value that will be used for calculating the open circuit voltage is taken to be at standard room temperature ($T_0 = 25$ C). The open circuit voltage variation with different temperatures (V_T) can be calculated as follows [25]:

$$V_T = V_{oc} + \frac{-44.43 \text{ J}/(\text{mol} \cdot \text{K})}{2(96400)} (T - T_0) \quad (9)$$

The voltage and current response can be characterized using the polarization curve shown in Figure 8. The polarization curve represents the maximum cell voltage and the drop in voltage as the current density is increased. The voltage losses are divided into three types: Activation losses, ohmic losses and concentration losses.

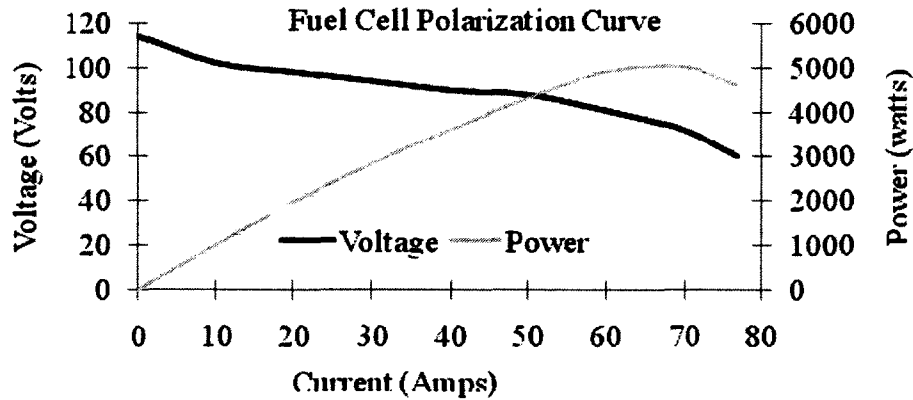


Figure 8: Fuel cell polarization curve

Ohmic losses are associated with the material resistance to transfer charge. Two ohmic losses are considered, the polymer membrane resistance to transfer ions and the electrodes resistance to transfer electrons to the load circuit. The ohmic loss represents the linear part of the polarization curve, thus, it can be represent using ohms law with a constant resistance, which is estimated to be $R=0.07565$ ohms for this work [26].

The Activation voltage loss is associated with the energy loss required to initiate the reduction and oxidation reactions at the fuel cell anode and cathode. Normally, the activation losses are dominant at lower current density levels. The physical nature of the activation voltage loss can also be explained at a microscopic level of the electrochemical

reaction that occurs at the electrode surface. The separation of electrons and ions results in the accumulation of electrons (negative charge) between the electrode and the electrolyte on the anode side, while ions (positive charge) build up on the cathode side. This physical phenomenon is known as the electrical double layer, it is very important to consider when modeling fuel cell behavior because in order to transfer the positive charge through the electrolyte, a voltage drop is required, and this voltage drop is the activation voltage loss. The activation voltage loss (V_{act}) is calculated using the Tafel equation [25]:

$$V_{act} = \frac{RT}{2\alpha F} \ln \left(\frac{i_{fc}}{i_0} \right) \quad (10)$$

Where, R is the universal gas constant, T is the temperature, α is the charge transfer coefficient; i_{fc} is the current drawn from the fuel cell and i_0 is the exchange current density. The exchange current density depends on the electrolyte and electrode material, in the case of PEM fuel cells, the electrolyte is a polymer while the electrode is a porous carbon plate containing platinum catalyst. For this of electrolyte-electrode combination, the exchange current density is estimated as:

$$i_0 = A_{fc}(5 \times 10^{-4}) \quad (11)$$

Where, A_{fc} is the fuel cell active area.

The concentration loss is associated with the change in fuel and oxidant concentration as their flow rates increase. The concentration voltage loss (V_{conc}) is dominant at higher current density levels. The voltage loss due to change in concentration is evaluated by considering the partial pressures of the reactant gases (p_{H_2} , p_{O_2}) [25]:

$$V_{conc} = \frac{RT}{2F} \ln \left(\frac{1}{p_{H_2} p_{O_2}^{1/2}} \right) \quad (12)$$

The partial pressures are calculated based on the purity of the fuel and air fed to the fuel cell ($x\%$, $y\%$), and also the rate of utilization of hydrogen and oxygen gasses (U_{H_2} , U_{O_2}):

$$p_{H_2} = (P_{fuel})(x\%)(1 - U_{H_2}) \quad (13)$$

$$p_{O_2} = (P_{Air})(y\%)(1 - U_{O_2}) \quad (14)$$

Knowing the fuel cell demand current, the number of cells in the stack (N) and the molar masses of hydrogen and oxygen (M_{H_2}, M_{O_2}), the mass flow rates ($\dot{m}_{H_2}, \dot{m}_{O_2}$) in kg/s can be calculated as follows [25]:

$$\dot{m}_{H_2} = \frac{N(i_{fc})(M_{H_2})}{2F} \quad (15)$$

$$\dot{m}_{O_2} = \frac{N(i_{fc})(M_{O_2})}{2F} \quad (16)$$

The hydrogen fuel and oxidant utilization rates are defined as [25]:

$$U_{H_2} = \frac{\text{Fuel Consumption Rate}}{\text{Fuel Supply Rate}} = \frac{N(i_{fc})(M_{H_2})}{(2F)(\dot{m}_{fuel})(x\%)} \quad (17)$$

$$U_{O_2} = \frac{N(i_{fc})(M_{O_2})}{(2F)(\dot{m}_{air})(y\%)} \quad (18)$$

3.1.2 DC/DC Voltage Converter

In order to accommodate for the fuel cell voltage drop, a DC/DC converter is used to maintain a constant voltage output while varying the output current. The converter used is a current controlled buck converter (i.e. the fuel cell voltage is reduced to match the DC bus voltage). The model for the DC-DC converter is obtained from the circuit diagram shown in Figure 9.

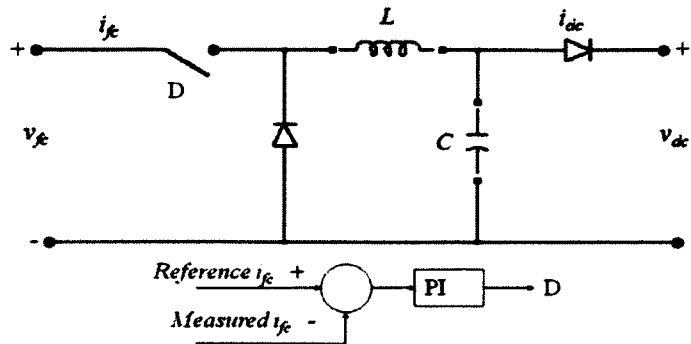


Figure 9: DC/DC voltage converter circuit

The main components of a DC-DC converter are a transistor switch and two energy storage elements a capacitor and an inductor. The basic principle of operation can be summarized by two states of the transistor: Open and Closed. When the switch is closed the circuit is shorted and thus the input voltage is not isolated from the load and current can only flow to the inductor and so its energy level increases. When the switch is opened on the other hand, the inductor discharges its energy to the to the capacitor across the load terminals As the transistor switch is opened and closed constantly at a certain duty cycle rate, the output voltage of the converter becomes a function of the duty cycle of the transistor switch and the input voltage of the converter. The relationship between the input and output voltage is:

$$\frac{V_{\text{Out}}}{V_{\text{input}}} = D \quad (19)$$

Where, D is the duty cycle. The above circuit can be modeled by writing the voltage loop equations for the case when the IGBT switch is open and when it is closed, thus the governing equations are:

$$\frac{dV_c(t)}{dt} = \frac{1}{C} (i_L - i_{\text{load}} - i_L d_D) \quad (20)$$

$$\frac{di_L(t)}{dt} = \frac{1}{L} (-V_c + V_c d_D + V_{\text{FC}}) \quad (21)$$

Where, V_c is the voltage across the capacitor, i_L is the current through the inductor, i_{load} is the current drawn by the load. The above equations were used to implement a mathematical model in the MATLAB/Simulink environment.

3.1.3 Lithium Battery Model

The battery is modeled based on the equivalent electric circuit model shown in Figure 10. In this model, the battery electrical behavior is represented using two basic elements, a resistor and a voltage source. The resistor element represents the internal resistance of the battery. The internal resistance takes into account several fundamental phenomena in battery chemistry. These phenomena are ohmic resistance (in the electrolyte, electrodes and battery terminals), the charge-transfer resistance associated

with the reactions taking place at the electrodes, and the diffusion resistance which has to do with the transport of reactants and products between the electrodes and the electrolytes. More complicated models already exist in literature that take into account the double layer capacitance effect by adding a capacitor element in parallel with the resistor element in the equivalent circuit model. However, for the purpose of designing a control based model, the capacitance effect will be ignored, as it has little impact on the controller design. The overall voltage output at the battery terminal as a function of the state of charge of the battery (SOC) is determined by subtracting the internal resistance voltage loss from the open circuit voltage of the battery (V_{oc}):

$$V_{Batt}(SOC) = n_s(V_{OC}(SOC) - IR_i(SOC)) \quad (22)$$

Where, n_s is the number of battery cells in series.

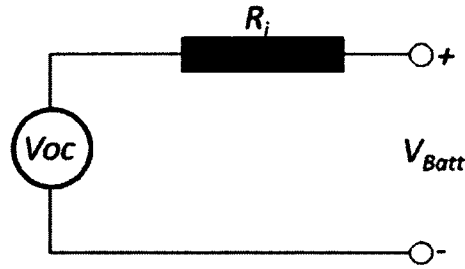


Figure 10: Battery equivalent circuit model

The open circuit and the internal resistance as a function of the SOC are typically determined by experimentally testing the battery cells. In a study to develop a mathematical model for lithium iron phosphate batteries, Khateeb et al. [27] performed discharge tests on a Lithium battery cell in order to develop a relationship between the battery depth of discharge (SOC), the open circuit voltage and the internal resistance. The experimental results were curve fitted and the voltage drop across the battery terminals is represented using the following equations:

$$R = 0.20139 + 0.58863(1 - SOC) - 0.81697(1 - SOC)^2 + 0.79035(1 - SOC)^3 \quad (23)$$

$$V_o = 3.95587 - 1.42918(1 - SOC) + 2.83095(1 - SOC)^2 - 3.7497(1 - SOC)^3 \quad (24)$$

Obtaining accurate SOC measurements is very critical in order to obtain an accurate battery model and to design a proper management system. The SOC is defined as the “ratio between the difference of the rated capacity and the net amount of charge discharged from a battery since the last full SOC on the one hand, and the rated capacity on the other hand” [28]. Several methods have already been developed for estimating the SOC, some of these methods are: discharge tests, coulomb counting and the Kalman filter. The advantages of each method vary depending on the application. For example, the Kalman filter method is more accurate, but requires more computational power and a more accurate mathematical model of the battery. The coulomb counting method is the most used method currently, and it gives fairly good accuracy. However, it requires accurate battery current measurements. In this work, the battery SOC is estimated using the coulomb counting method. This method requires consistent measurements of the battery discharge/charge current. The battery current is then integrated over the time period that the current is discharged/charged from the battery. The SOC is then calculated as follows:

$$\text{SOC}(t) = 1 - \frac{\int i dt}{Q(\text{Ah})} \quad (25)$$

3.1.4 Vehicle Model

Since the main goal for modeling the vehicle is to capture the transient vehicle load demand, the vehicle model considered is a two dimensional model. The vehicle is modeled using the simple longitudinal vehicle dynamics equations, where the total road loads acting on the vehicle are calculated based on the aerodynamic drag, rolling resistance, acceleration and road grade loads. The vehicle parameters used in the mathematical model are shown in Table 3. In order to simplify the mathematical model, there are several assumptions that were made in regards to the vehicle dynamics aspects. These assumptions can be summarized as:

- Dynamic effect of weight distribution are not considered for the rolling resistance calculations

- Rolling resistance is assumed to be distributed equally on all tires (assumes front and rear tires have the same tread pattern and size)
- Rolling resistance and aerodynamic drag are assumed to be perpendicular to the direction of vehicle velocity
- Only the frontal area of the vehicle is considered when calculating the aerodynamic drag on the vehicle
- The inertial forces due to the rotating parts in the vehicle are not included in the calculations

Table 3: Vehicle parameters [23]

Vehicle mass (m)	308.45 kg
Frontal area (A)	0.9 m ²
Drag coefficient (C _d)	0.6
Rolling coefficient (C _r)	0.014
Air density (ρ)	1.204 kg/m ³
Wheel radius (r)	0.1397 m
Top Acceleration (a)	1.9637 m/s ²

Given these simplifications, the mathematical equations that describe the road loads can be expressed as:

$$F_{\text{Total}} = F_{\text{Rolling}} + F_{\text{Drag}} + F_{\text{Gradient}} + F_{\text{acceleration}} \quad (26)$$

$$F_{\text{Rolling}} = mgC_r \cos\theta \quad (27)$$

$$F_{\text{Drag}} = \frac{1}{2} \rho C_d V^2 \quad (28)$$

$$F_{\text{Gradient}} = mg \sin\theta \quad (29)$$

$$F_{\text{acceleration}} = ma \quad (30)$$

Where; V, a, and ω are the vehicle velocity (m/s) and acceleration (m/s²). The electric motor drive is modeled based on its characteristic curve and efficiency maps

shown in Figure 11 and Figure 12. The motor and controller parameters are determined based on estimates provided by the motor manufacturer.

AC Motor Characteristics

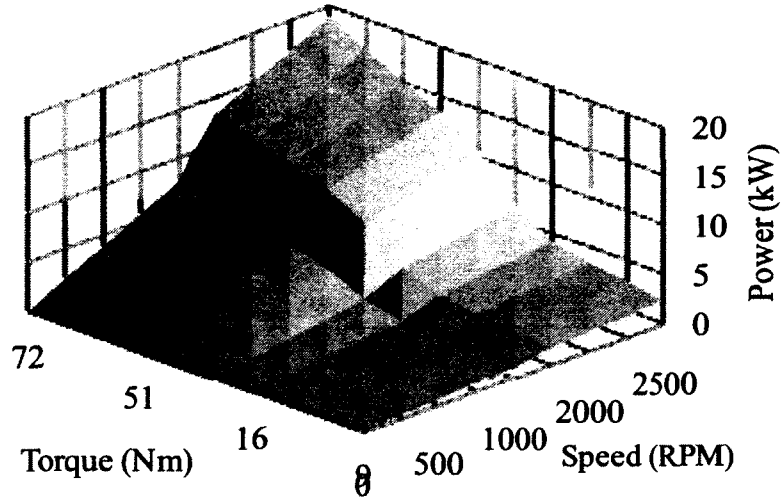


Figure 11: AC Motor characteristics

AC Motor Efficiency

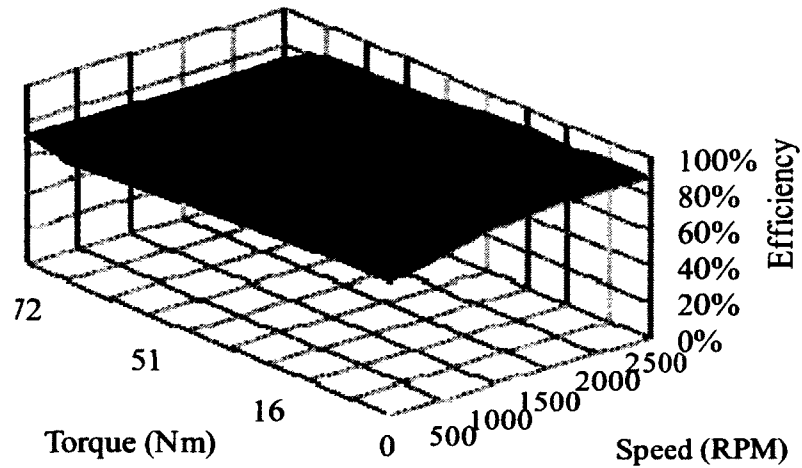


Figure 12: Motor efficiency map

3.2 Controller design

3.2.1 Modes of Operation

Based on the road loads, and SOC of the battery stack, the hybrid powertrain operation can be characterized by three main operation modes. These operation modes are: hybrid drive, charge sustaining, and regenerative braking. At any time the operation

of the hybrid powertrain by one or a combination of these modes. The modes of operation are illustrated in Figure 13.

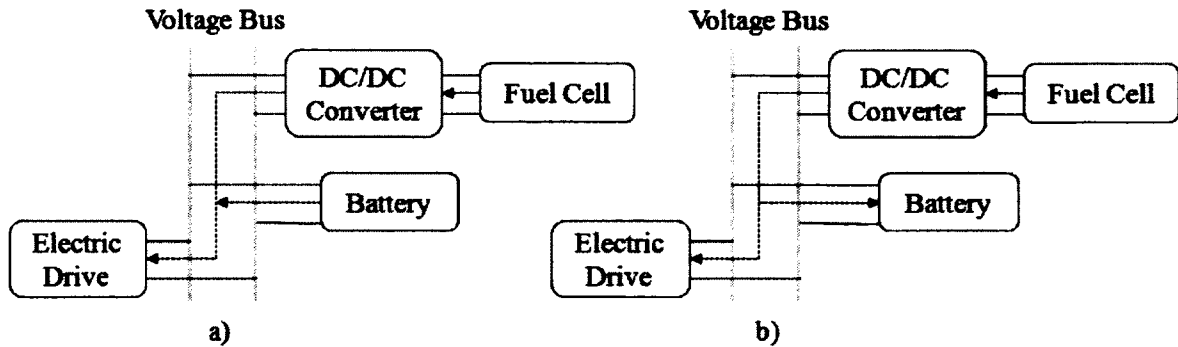


Figure 13: Modes of operation: a) hybrid drive b) regen/charge sustaining

At each operation mode, the power management controller adjusts the contribution of the fuel cell and battery in the hybrid powertrain. The power split between the battery and the fuel cell can be defined by the degree of hybridization (DOH), which is normally used as the ratio between the rated powers of the fuel cell to the rated drive power when sizing the vehicle components. However, in this project the term DOH is used to refer to the instantaneous power split between the fuel cell and battery. DOH is defined as:

$$\text{DOH} = \frac{\text{Instantaneous Power Supplied by Fuel Cell}}{\text{Instantaneous Power Demand}} \quad (31)$$

The instantaneous power demand by the vehicle electric drive is determined by knowing the vehicle speed and torque required at the wheels:

$$P_{\text{drive}} = (\text{Torque})(\text{Speed}) \quad (32)$$

The torque at the wheels is normally not a measured parameter, and cannot be determined unless the road loads are known ahead of time. However, it is directly related to the driver pedal command, where it represents the driver's response to two factors: the resistance force and the desired speed, in other words, the driver will either press or release the pedal depending on how fast he/she wants to drive and also how much resistance force (air drag, rolling drag and gravity) the vehicle is facing. The pedal

position is determined using the classic cruise control example, where a PID controller is used to adjust the driver "pedal position" from -1 to 1 depending on how well the vehicle is matching the command speed. Physically, a pedal position from 0 to 1 represents the driver using the accelerator, while a pedal position from 0 to -1 represents the driver using the brake. Using this simple controller, the pedal position at each speed command is determined and the requested torque is calculated by multiplying the pedal position by the rated vehicle torque as shown in Figure 14. Thus, DOH can be determined instantaneously during the drive cycle. The value of DOH will vary depending on the mode of operation and control method used. If the powertrain is in hybrid/charge sustaining mode, then DOH will vary from 0 – 1 depending on the power split between the fuel cell and the battery. If the powertrain is in regenerative braking mode, DOH will be zero.

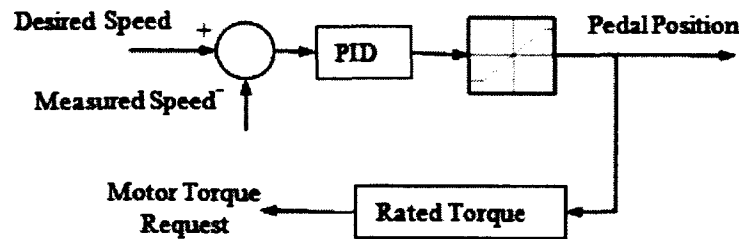


Figure 14: Pedal position

3.2.2 Constraints

The main constraints on the power management controller are related to the life of the fuel cell and the battery. As discussed in the introduction, fuel cells have trouble dealing with high transient demands. In fact, it has been shown experimentally that frequent high rate current demands can damage the fuel cell and significantly reduce its expected life. Thus, the rate of current request sent to the fuel cell has to be subjected to limitation. The exact rate limit value is determined based on previous studies [29], and is selected to be $\pm 2 \text{ A.s}^{-1}$.

The second constraint is related to the battery life and thus its SOC level and operating range. The battery must at all time have enough capacity to recover energy from regenerative braking. Based on the driving cycle and the rated deceleration of the

SAE Baja vehicle, it was determined that there must be at least 10% of the battery capacity room available for storing regenerative energy. Thus, the battery SOC must at all time be less than 90%. However, as was discussed previously, the average operating SOC of lithium ion batteries impacts the degradation of the battery capacity over time, and so the range must be selected to prolong the battery life. Several research studies have done experimental testing in order to find the ideal operating range for the battery [30]. Based on these studies it was decided that the battery SOC would be maintained at an average value of 60%.

3.2.3 PID Controller

The ultimate goal in this control method is to monitor and maintain the state of charge of the battery at its nominal value of 60 %. In the case where the SOC of the battery drops significantly below the reference value, a current request is sent to the fuel cell in order to charge the battery. The magnitude of fuel cell current request is also controlled by the power needed to drive the vehicle. Thus, in order to satisfy both the battery SOC and the vehicle power demand, two control loops are required; a battery current control loop and a fuel cell current control loop. A PID controller is used to compare the calculated SOC with a reference value to generate a battery current demand signal. This generated signal is then used as a reference value for the battery current. Another PID controller is then used to generate a fuel cell current demand based on the difference between the battery current and its reference value. The controller is explained by the diagram in Figure 15.

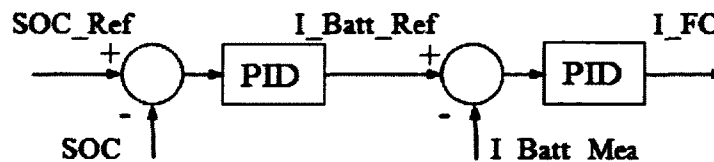


Figure 15: PID Controller diagram

3.2.4 Fuzzy Logic Controller

The two input variables to the fuzzy logic controller are the pedal position and the SOC of the battery. Similar, to the PID controller, the fuzzy logic controller aims at

maintaining the SOC at nominal level, for this reason the first control input to the fuzzy logic controller is the SOC of the battery. The second input variable is selected to be the driver pedal position. The output variables of the fuzzy controller are chosen to be the degree of hybridization (DOH), and also battery recharge current supplied from fuel cell (FC Current). While, normally DOH is used when sizing the vehicle components, it is used in this controller as the main output control variable. The value of DOH ranges from 0 to 1, with 0 representing a full battery vehicle (powered by battery only) and 1 representing a full fuel cell vehicle (powered by fuel cell only). Thus, DOH represents the fraction of power that the fuel cell contributes to the overall vehicle power demand. Once the DOH is determined from the controller, it is multiplied by the required vehicle power to obtain the required fuel cell power. A lookup table is then used to convert the power requirement into current requirement. The controller block diagram is shown in Figure 16.

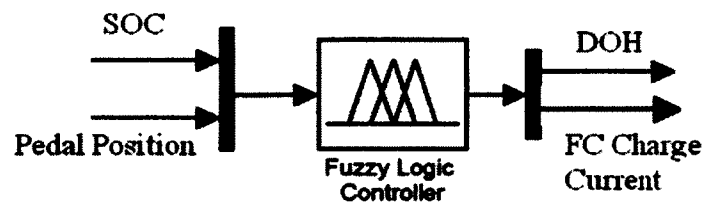


Figure 16: Fuzzy logic controller

Before choosing the membership functions, specific test cases were run using the simulation model in MATLAB in order to determine how the overall system efficiency is affected by different degrees of hybridization. The test cases are: acceleration (0 - 25 km/h in 3.5 seconds), deceleration (25 - 0 km/h in 3.5 seconds), driving at constant speed (30 km/h) and hill climb (10 degrees grade). The results from the acceleration and deceleration tests are shown in Figure 17.

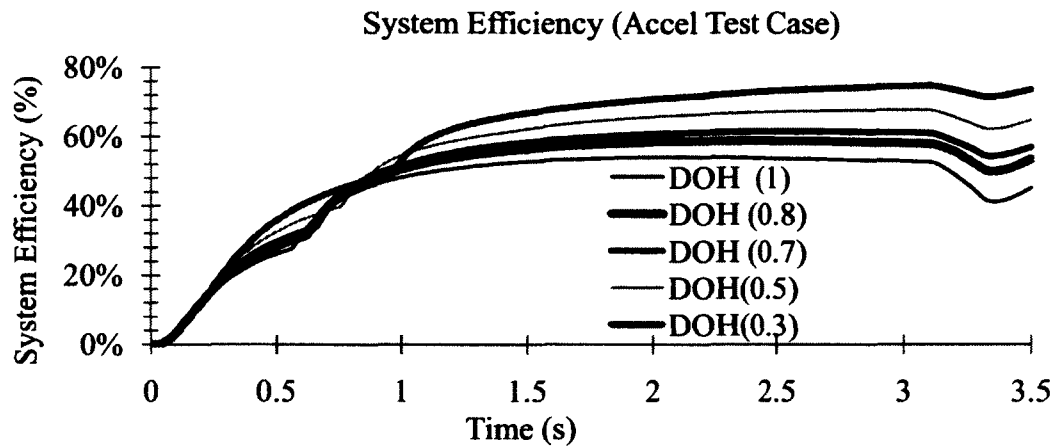


Figure 17: Acceleration efficiency test cases

It is clear to see that the DOH has a significant impact on the overall system efficiency, where the efficiency improves as the fuel cell power contribution is reduced (i.e. the DOH decreases). Thus, the range and categories of the DOH membership functions can be selected based on that. The membership functions for DOH are shown in Figure 18, where it is classified into three modes of operation: Low, Medium and High. The medium mode of operation was chosen to cover the largest span of possible DOHs, and thus reducing the fuel cell's transient response.

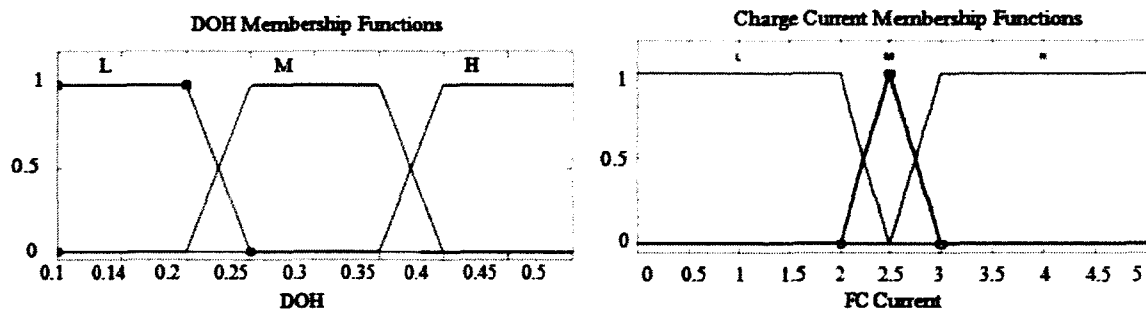


Figure 18: Output membership functions

The second output variable is the fuel cell charging current (FC Current), this variable is strictly dependent on the SOC of the battery and is not impacted by the vehicle power demand. The membership functions for FC Current are shown in Figure 18, where it is divided into three levels: L (Low), M (Medium) and H (high) ranging from minimum 0 amps to maximum 5 amps. The membership functions for the SOC and pedal position

input variables are shown in Figure 19. The SOC of the battery is classified into three main categories Low, Medium and High to correspond to a nominal SOC of 60 %. The pedal position on the other hand is varied from -1 to 1, where all negative values are categorized as "regen" mode and the positive values are divided into 4 sections: quarter, half, three quarters and full pedal displacement.

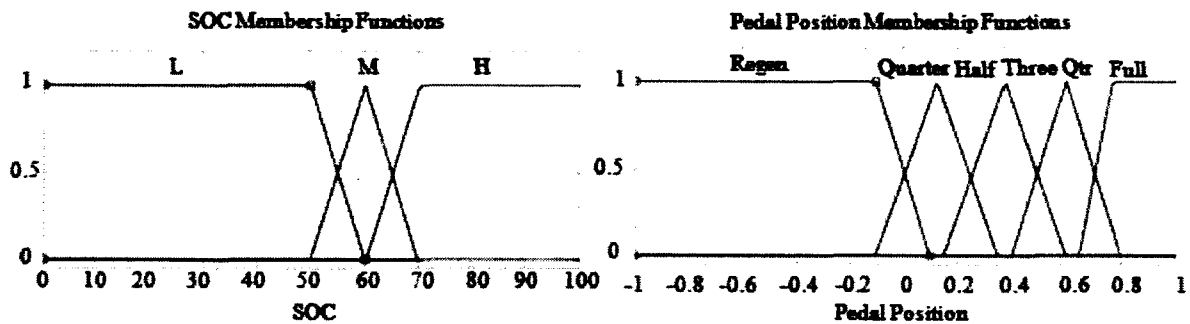


Figure 19: Input membership function

The output of the controller is determined by a set of “if-then” statements based on the linguistic definition of the membership functions. For example if the SOC is in the “L” low range, then regardless of the pedal position, the DOH output of the controller will be in the “H” high range. The output of the controller is shown in Figure 20.

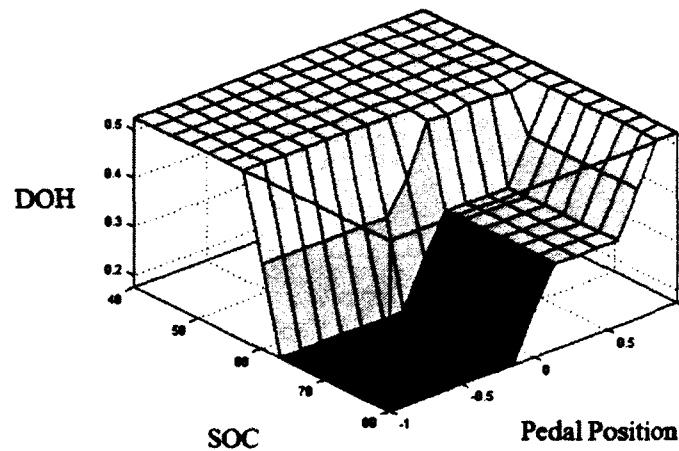


Figure 20: Surface plot of the fuzzy logic controller output

3.2.5 Optimization approach

The problem of designing a power management strategy for hybrid vehicles can be formulated into an optimization problem, in which the cost function is the fuel

consumption. However, as mentioned in the introduction, global optimizations are not feasible due to the need to know the driving cycle ahead of time. Thus, a local optimization will be used instead. The local cost function is based on the fuel flow rate supplied by the fuel cell. Since in the hybrid fuel cell-battery vehicle all of the energy supplied essentially comes from the hydrogen fuel, the energy withdrawn from both sources must be converted into equivalent hydrogen fuel flow rate. This was accomplished as follows:

$$\dot{m}_{eq} = \dot{m}_{fc} + c(\dot{m}_{batt}) \quad (33)$$

The fuel cell and battery equivalent fuel mass flow rates are defined using the higher heating value of hydrogen (141.9×10^6 J/kg):

$$\dot{m}_{batt} = \frac{i_{batt} V_{batt_OC}}{141.9 \times 10^6 \text{ J}} \frac{1}{\text{Eff}_{fc} \text{Eff}_{batt}} \quad (34)$$

$$\dot{m}_{fc} = \frac{i_{fc} V_{fc}}{141.9 \times 10^6 \text{ J}} \frac{1}{\text{Eff}_{fc}} \quad (35)$$

Where, Eff_{fc} and Eff_{batt} are the fuel cell and battery efficiencies respectively. The fuel cell efficiency is obtained by a lookup table from the manufacturer, while an average value is used for the battery efficiency. Another parameter that must be included in the optimization is the SOC of the battery. In order to incorporate the SOC of the battery in the optimization problem, the battery equivalent fuel flow rate is multiplied by a variable factor “c”. This variable is varied between 0 – 2 depending on the SOC of the battery and can be defined as follows:

$$c = 1 - \frac{\left(\text{SOC} - \frac{\text{SOC}_{max} + \text{SOC}_{min}}{2} \right)}{\frac{\text{SOC}_{max} - \text{SOC}_{min}}{2}} \quad (36)$$

The value of c essentially manipulates the total fuel flow rate depending on the SOC of the battery. By doing so, the optimized power split will be high enough to take into account charging the battery when the SOC is too low, or discharging it when the SOC is too high. The relationship between “c” and the SOC is summarized as:

If SOC = 40, then c = 2

If SOC = 50, then $c = 1.5$

If SOC = 60, then $c = 1$

If SOC = 70, then $c = 0.5$

If SOC = 80, then $c = 0$

In this equation, SOC_{max} and SOC_{min} are the maximum and minimum allowed SOC of the battery. As mentioned in section 6.2, the average SOC will be maintained at 60%, thus, SOC_{max} and SOC_{min} are 80% and 40% respectively.

This optimization problem is solved without using any complex mathematical algorithm; instead a simple for-loop is used to find the least hydrogen fuel flow rate while varying the requested power to drive the vehicle from 0 – 3000 Watts and the SOC in the range between 40% to 80%. The result shown in Figure 21 is a relationship between the requested power, the SOC of the battery and the DOH, which can be implemented in the controller as a two dimensional lookup table.

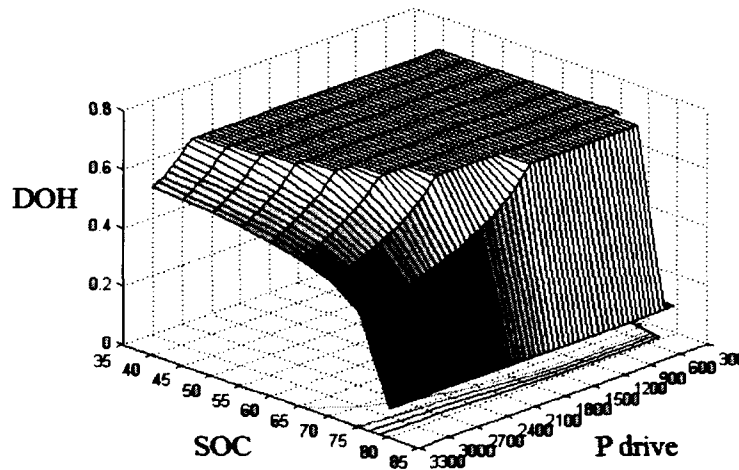


Figure 21: Fuel flow rate optimization surface plot

Figure 21 shows that most of the time the optimal fuel flow rate is achieved if the DOH is highest, i.e. if the fuel cell is used as the main power source with minimal supply from the battery. This comes as no surprise since the most efficient way to transfer hydrogen power to the electric drive is by going directly from the fuel cell. However, that is not always true since maintaining the SOC of the battery between 80%-40% is a

control objective. Thus, it can be seen that as the battery SOC is increased, the DOH becomes smaller favoring the battery over fuel cell in order to bring down its SOC, on the other hand, as the SOC is decreased below its average, the DOH becomes higher to recharge the battery. In addition to that, the efficiency of the fuel cell varies as the power request is increased, this also plays into finding the most optimal DOH, and can be seen in the variation of DOH as power request is increased. To summarize the method of local optimization is implemented varying the degree of hybridization parameter DOH to find the value that minimizes the equivalent fuel flow rate. The values of DOH are varied between 0.1 (minimal fuel cell usage) to 0.9 (maximum fuel cell usage) instantaneously at each power request from the electric drive. The process is illustrated in the flow chart shown in Figure 22.

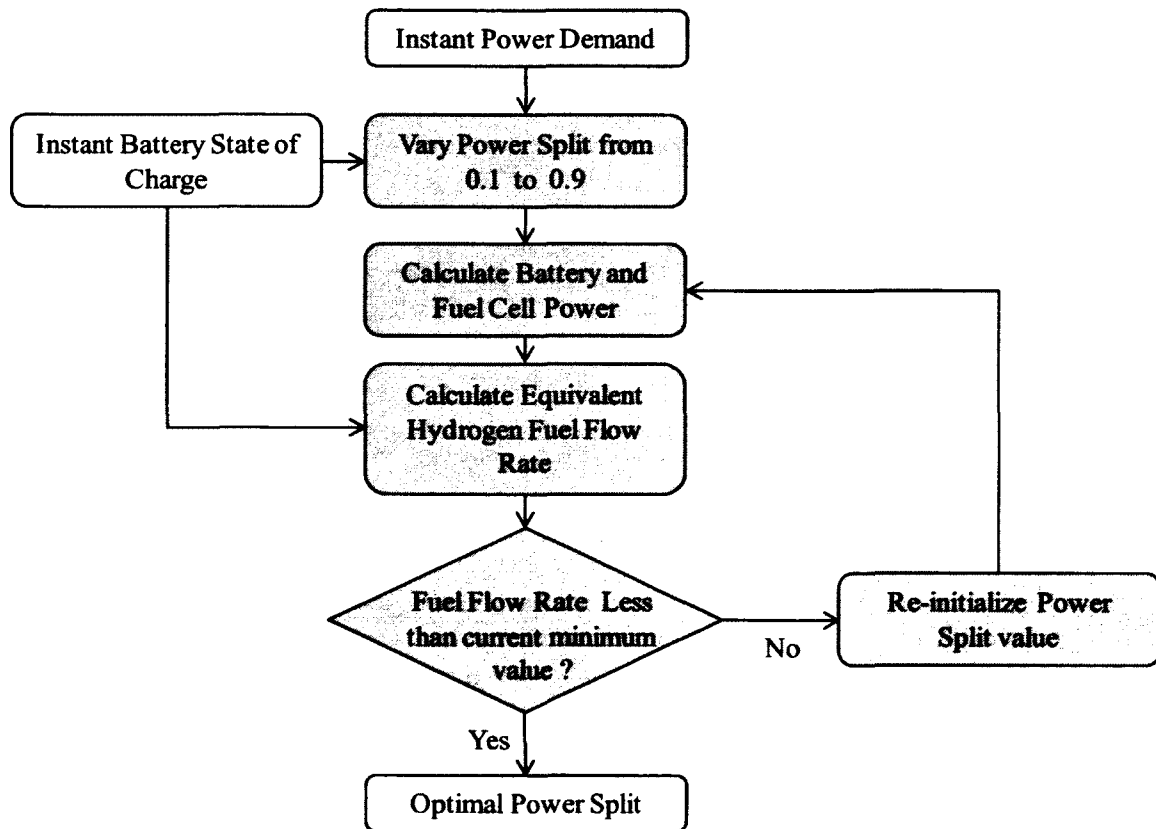


Figure 22: Optimization approach flow chart

3.3 Performance measures

3.3.1 System Efficiency

In this study, the efficiency and transient response of the fuel cell are considered the main performance measures. The fuel cell and battery efficiencies are defined as follows:

$$\text{Eff}_{\text{FC}} = \frac{I_{\text{FC}} V_{\text{FC}}}{(\dot{m}_{\text{H}_2})(\text{HHV}_{\text{H}_2})} \quad (37)$$

$$\text{Eff}_{\text{Batt}} = \frac{V_{\text{Batt}}}{V_{\text{Batt_OC}}(\text{SOC})} \quad (38)$$

Where, \dot{m}_{H_2} is the hydrogen fuel mass flow rate (kg/s), HHV_{H_2} is the higher heating value of hydrogen fuel (141.9 MJ/Kg), V_{Batt} is the measured battery voltage at its terminals, and $V_{\text{Batt_OC}}(\text{SOC})$ is the open circuit voltage as a function of the state of charge of the battery. Thus, the overall system efficiency can be derived using the following "If-Else" statements:

If power demand > 0, then:

$$\text{Eff}_{\text{system}} = \frac{P_{\text{drive}}}{(\dot{m}_{\text{H}_2})(\text{HHV}_{\text{H}_2}) + (I_{\text{Batt}})(V_{\text{Batt_OC}}(\text{SOC}))/\text{Eff}_{\text{FC}}\text{Eff}_{\text{DC}}} \quad (39)$$

Else, if power demand < 0, then:

$$\text{Eff}_{\text{system}} = \frac{|(I_{\text{Batt}})(V_{\text{Batt_OC}}(\text{SOC}))|}{(\dot{m}_{\text{H}_2})(\text{HHV}_{\text{H}_2}) + |P_{\text{drive}}|} \quad (40)$$

Else, if battery power < 0, then:

$$\text{Eff}_{\text{system}} = \frac{P_{\text{drive}} + |(I_{\text{Batt}})(V_{\text{Batt_OC}}(\text{SOC}))|}{(\dot{m}_{\text{H}_2})(\text{HHV}_{\text{H}_2})} \quad (41)$$

3.3.2 Fuel Consumption

In addition to the overall system efficiency, the miles per gallon of gasoline equivalent (MPGGE) is also an important measure that gives an insight as to how the fuel cell vehicle compares to internal combustion engine vehicles in terms of its fuel consumption. The conversion to the equivalent miles per gallon of gasoline is done on the

basis of the hydrogen fuel energy content compared to the gasoline energy content. The energy content of liquid gasoline fuel is 115,000 BTU per gallon, while the energy content of gaseous hydrogen fuel is 113,738 BTU per kilogram, thus, the energy in one gallon of gasoline is equivalent to that in 1.012 kilogram of hydrogen fuel. Therefore, the MPGGE is calculated as follows:

$$\text{MPGGE} = \left(\frac{\text{Miles}}{\text{kg of H}_2} \right) \left(1.012 \frac{\text{kg of H}_2}{\text{gallon of gasoline}} \right) \quad (42)$$

The total fuel mass consumed during a driving cycle can be calculated by integrating the fuel mass flow rate over the driving cycle time period. However, in order to accurately measure the amount of fuel consumed for the entire driving cycle, the initial and final state of charge (SOC) of the battery must also be taken into consideration. In other words, if the battery is assumed to have a 60% initial SOC, then the amount of fuel required to recharge the battery back to its initial SOC must be considered when calculating the total fuel mass as shown in Eq.(16):

$$m_{\text{fuel consumed}}(t) = \int_0^t \dot{m}_{\text{driving}}(t) dt + m_{\text{recharge}}(t) \quad (43)$$

The second term (m_{recharge}) in the equation above, represents the fuel mass required to recharge the battery back to its initial state of charge. This term is determined by first calculating the amount of energy required to recharge the battery from its final SOC to its initial SOC:

$$\Delta E_{\text{recharge}}(t) = [Q(\text{SOC}(t) - \text{SOC}_i)]V_{\text{nom}} \quad (44)$$

Where, $\Delta E_{\text{recharge}}$ is the energy in Watt-Hour, Q is the rated battery capacity in Ampere-Hour, V_{nom} is the nominal battery voltage, $\text{SOC}(t)$ is the final state of charge, and SOC_i is the initial state of charge. Then, the total hydrogen mass consumed in recharging the battery can be calculated using the hydrogen fuel Higher Heating Value (141.9 MJ/Kg):

$$m_{\text{recharge}}(t) = \Delta E_{\text{recharge}}(t) \left(\frac{3600\text{s}}{\text{hour}} \right) \left(\frac{\text{Kg}}{141.9 \times 10^6 \text{ J}} \right) \left(\frac{1}{\text{Eff}_{\text{batt}} \text{Eff}_{\text{FC}}} \right) \quad (45)$$

Where, Eff_{batt} and Eff_{FC} are the battery and fuel cell efficiencies at the final SOC of the battery.

3.3.3 Battery Cycling

As stated in the objectives section, one of the main design goals of the hybrid fuel cell vehicle controller is to operate the powertrain in a way that prolongs the battery life. The main function of the battery in the hybrid vehicle powertrain is to recover the regenerative braking energy and also supply the pulse power demand that the fuel cell cannot handle. Thus, the battery will be forced to go through a high number of charge/discharge cycles depending on the driving cycle considered. These charge/discharge cycles however, are referred to as “partial state of charge” cycles. Although lithium ion batteries do not suffer from “memory effect” (loss of capacity as a battery is charged after partial discharge) like nickel cadmium batteries, the number of partial SOC cycling has an impact on the battery degradation process. Kato et al [30] developed an experimental procedure for testing the effect of partial SOC cycling on lithium ion degradation process. It was shown that although the degradation greatly depends on the operating temperature, it was greatest as the number of partial cycles increased at an average SOC of 75% and smallest at average SOC of 50%. The degradation increased again at an average SOC of 25%.

The impact of the control algorithm on the battery life is somewhat indirect, since the control algorithm dictates the fuel cell current command only, and by changing the fuel cell current, the battery current changes accordingly to supply more or less current to the voltage bus. Thus, the battery life cannot be taken into consideration directly when designing the control algorithm; however, it can be used as a performance measure once the controller is designed. Consequently, the ability to predict battery life and degradation becomes a very important topic, but it is also a very complex problem that researchers still do not have an answer for, mainly due to the different processes and stress factors that take place in batteries as they age. Several research works have attempted to solve this problem using experimental data or artificial neural network

modeling [31], [32], however, neither is applicable in this project do to the lack of battery data. For that reason, the main performance measure will be the number of battery charge/discharge cycles. Therefore, the controller that results in the least number of battery cycles will be deemed most appropriate to prolong the battery life.

For the case of the SAE Baja vehicle in this project, the vehicle model developed earlier was simulated with a battery only powertrain configuration, in order to examine the battery performance if it were to be used by itself without the fuel cell. The federal test procedure (FTP-72) drive cycle, also known as the Urban Dynamometer Driving Schedule (UDDS) [33], was used for testing the powertrain performance. This driving cycle is mainly used to simulate city driving conditions, where the vehicle is forced to accelerate and decelerate very frequently. The battery SOC during the FTP 72 cycle is shown in Figure 23, where the SOC decreases by 50%. Figure 24 shows the number charge/discharge cycles that the battery would have to go through if it were operated alone without the fuel cell, which means charge cycles are only a result of the regenerative braking, and not a charge sustaining control algorithm. The results obtained when operating the vehicle as a battery powered electric vehicle is used as a comparison standard when developing the power management controllers.

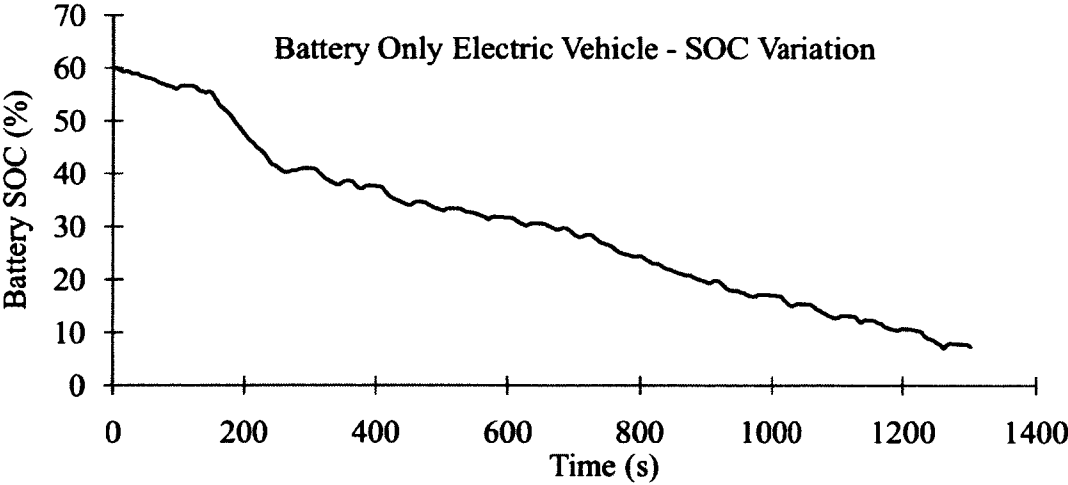


Figure 23: SOC - Battery only simulation

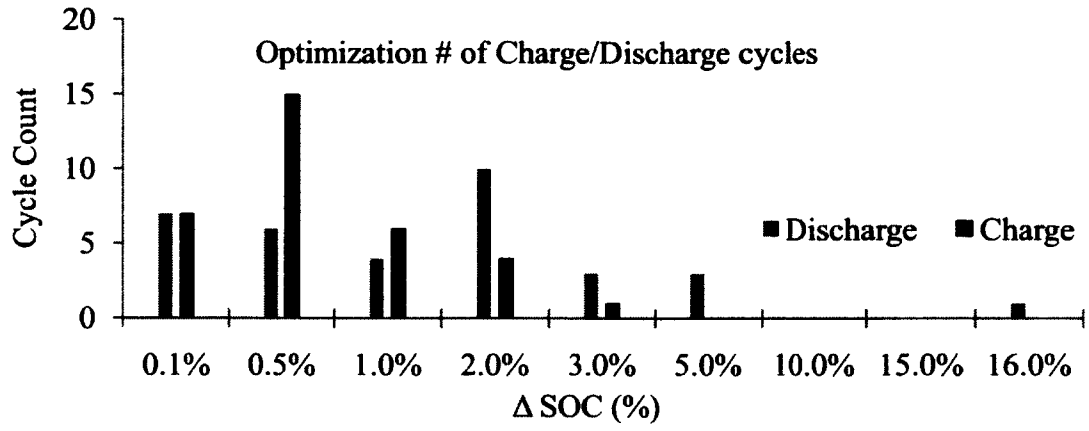


Figure 24: Discharge cycle count - Battery only simulation

CHAPTER IV. SIMULATION RESULTS

The Federal Test Procedure (FTP-72) drive cycle also known as the Urban Dynamometer Driving Schedule (UDDS) was used for testing the powertrain performance. This driving cycle is mainly used to simulate city driving conditions, where the vehicle is forced to accelerate and decelerate very frequently. Thus, it is suitable for this study, since the main goal is to improve the transient behavior of fuel cell powered vehicles. However, in order to accommodate the maximum speed of the SAE Baja vehicle (60 km/h), the drive cycle was scaled down by a factor of 1.5, resulting in a 20.63 km/h average speed over a distance of 8 kilometers driving cycle. The speed profile over time is shown in Figure 25.

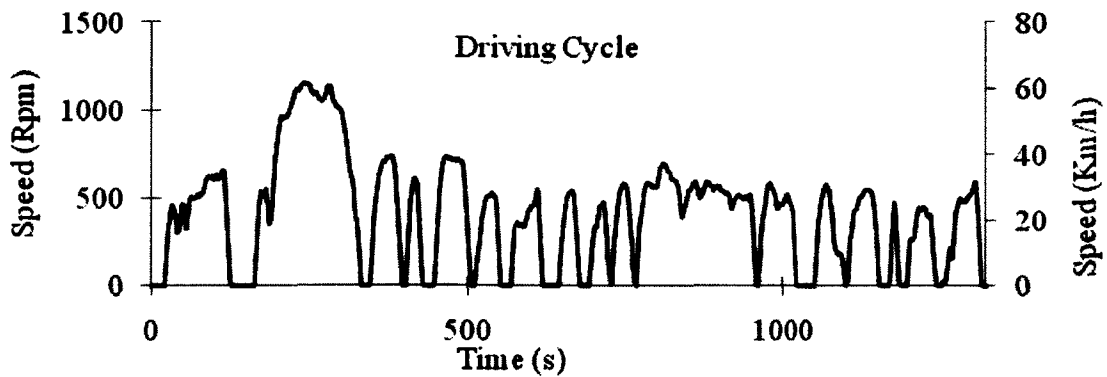


Figure 25: Simulation driving cycle

4.1 Power demand

The vehicle power demand and fuel cell power contribution for each control method are depicted in Figure 26. The transient power demand required to propel the vehicle through the driving cycle is satisfied; however, the fuel cell contribution varies in each control method. In general the fuel cell power contribution is limited by its transient constraints, and thus it is clear to see that the fuel cell power does not follow the vehicle power demand. The portion of the vehicle power demand not met by the fuel cell and the regenerative braking power are covered by the battery. Note that the battery power contribution is simply the vehicle power demand minus the fuel cell power contribution. The fuel cell power demands in each graph show the similarity between the optimization approach and the fuzzy logic approach, where both of these approaches use the variable

Degree of Hybridization (DOH) meaning the percentage of power demand covered by the fuel cell. The PID controller on the other hand is somewhat independent of the power demand and is more concerned with the SOC of the battery stack and thus, the fuel cell power profile does not follow the overall power demand profile as the other two controllers do.

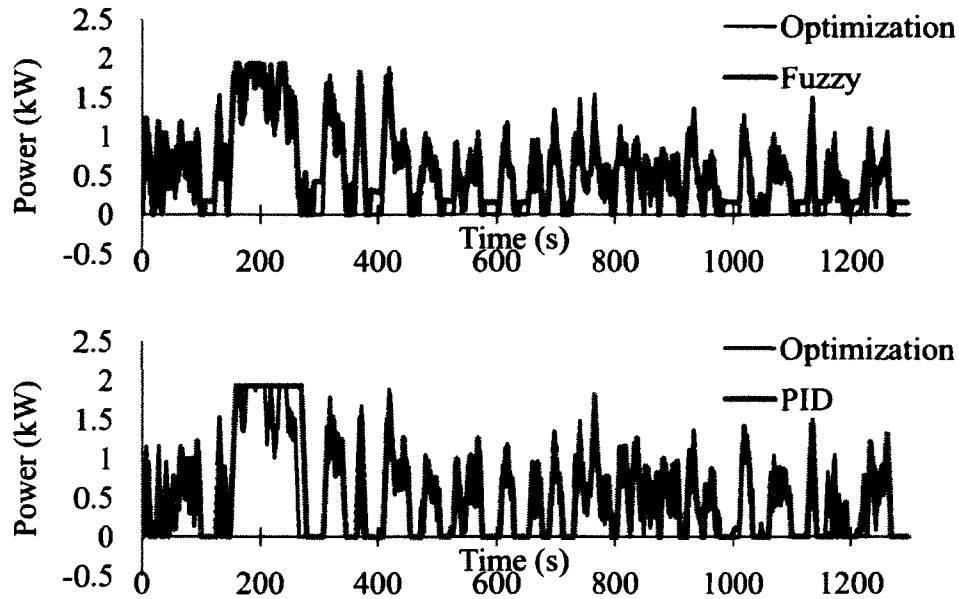


Figure 26: Simulation results: power demand

All three control methods allow the powertrain to meet the road load power demand. The main difference between each control method is the transient response of the fuel cell. It is desirable to have the fuel cell operate in a less transient manner and more steady state in order to prolong its life time. Comparing the response in Figure 26, the PID control method seems to operate the fuel cell in a more steady operation; however, the difference is not significant enough to have a major impact on the fuel cell operating time.

4.2 Battery SOC variation

The change in the battery SOC during the simulation is shown in Figure 27. Due to the fact that the simulation time is less than 30 minutes, the variation in the SOC is kept within 5%. However, it is clear to see the impact of the control strategy on the SOC.

Both the PID and fuzzy approaches are more charge sustaining than the optimization approach. The change in SOC shows how aggressive each control method is in maintaining the battery SOC. This is in fact the main difference between hybrid vehicle control strategies. Most control strategies operate around keeping the SOC closer to a previously defined value, in this case 60% is that value, however, keeping the SOC around that value implies more charging cycles for the battery, which as was discussed earlier contributes to the reduction of battery capacity over lifetime. In addition to that, charging the battery constantly will also have an impact on the total fuel consumption which is discussed in the next section. Thus, there is a tradeoff in the way the SOC is maintained that prolongs the battery life and also optimizes the fuel efficiency.

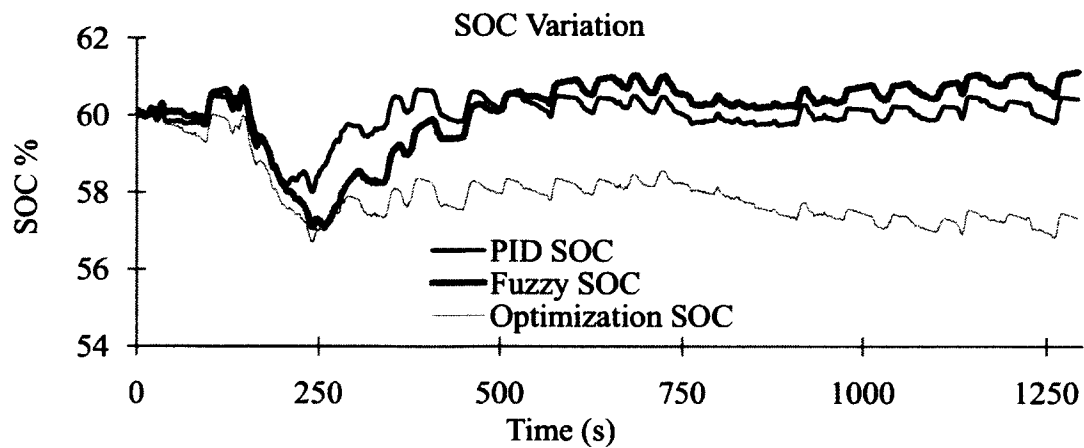


Figure 27: Battery SOC

Comparing the SOC variation between the control methods presented in this project (Figure 27), the PID and fuzzy logic methods are clearly more aggressive in maintaining the SOC of the battery, as it is closely kept near the nominal value of 60%. The optimization method is more flexible, because it is based on minimizing the fuel consumption as opposed to maintaining the battery SOC; however, it still keeps the battery SOC within an acceptable range.

The behavior of the battery SOC during the driving cycle gives insight on the general power management strategy using each control method. In general with the PID controller the battery stack is utilized as a load leveling power source to only buffer the

transient vehicle power demands and allow the fuel cell to operate at more steady state conditions. This can be seen in the SOC curve of the PID controller, where the battery experiences several spikes in the SOC (to accommodate transient demands that are too fast for the fuel cell), however, overall it is kept within a close range to the initial SOC. With the optimization approach on the other hand, the battery is utilized as a load following power sources used to share the total vehicle power demand with the fuel cell in order to improve the overall fuel consumption of the system. This can also be seen in the SOC response, where the battery in the optimization approach experiences the deepest decrease in the SOC. This indicates that the battery is sharing the total vehicle loads with the fuel cell, and not just handling the quick transient demands. Finally, the fuzzy logic approach is a simply a set of rules that dictate the operation mode of the system depending on the SOC of the battery and the total power being demanded by the electric drive. Thus the battery in the fuzzy logic control method is utilized in a combination of load leveling and load following, and therefore the SOC of the battery when using the fuzzy logic controller tends to fluctuate in between the optimization controller curve and the PID controller curve, which represent the “extremes”. The impact of the SOC strategy on the fuel consumption and the battery life are discussed in the next sections.

4.3 Fuel consumption

The next step is to compare the fuel consumption (in kg of H₂ fuel) of the vehicle over the 8 kilometers the vehicle travels in the FTP-72 driving cycle. Figure 28 and Table 4 summarize the amounts of fuel consumed using each control approach.

Table 4: Fuel consumption

	Distance Traveled	Total Fuel Consumed (kg)	H ₂ Density @ 35 MPA (kg H ₂ / L)	Gas Tank Volume (L)
PID Method	8 km	0.008920	0.014	0.6372
fuzzy Method	8 km	0.008875	0.014	0.6339
Optimization Method	8 km	0.008601	0.014	0.6144

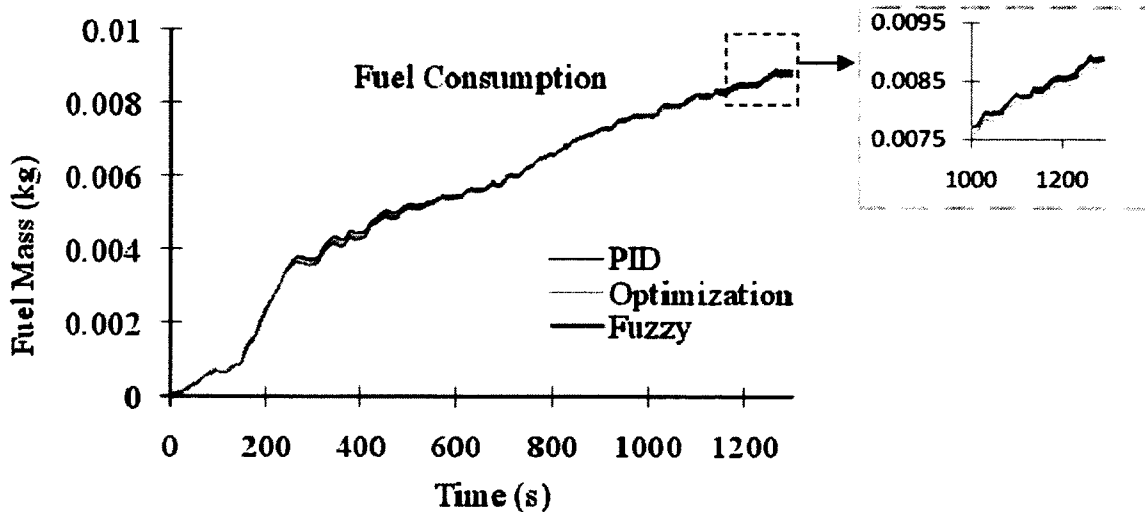


Figure 28: Fuel consumption

It is hard to make conclusions on which driving cycle is more fuel efficient based on this result due to the small difference in fuel consumed; however, if the storage tank volume is taken into consideration (assuming hydrogen is stored at 35 MPA) the optimization method saves approximately 20 mL to drive a distance of 8 km. Thus, if the vehicle is designed to have a driving range of 400 km for example, then the optimization control method would save approximately 1 liter of fuel storage room. This number can become even more significant when taking into consideration a midsize sedan or a van as opposed to the SAE Baja vehicle. The MPGGE for each case was also calculated, and it was determined that over the FTP driving cycle, the case with PID controller scores an MPGGE of 488, the case with fuzzy logic controller scores an MPGGE of 570.14, while, the one with optimization based controller scores an MPGGE of 585.35. In all cases the MPGGE calculation takes into account both fuel needed to drive the vehicle and the fuel needed to recharge the battery to its initial SOC. Note that the obtained MPGGE values are for the 308 kg Baja vehicle and this explains why they seem so high compared to actual road vehicles, for example the Honda FCX Clarity has a marketed MPGGE value of 72.8. Nonetheless, the MPGGE value gives a good comparison of the performance of each control methodology. Although, the difference is very small, it is clear to see, as expected, that the optimization method requires the least amount of fuel to get through the driving cycle.

The overall system efficiency curve for each control method is shown in Figure 29. In the case of a non-plug-in hybrid configuration, the system efficiency essentially corresponds to the fuel consumption since all energy comes from the hydrogen fuel. However, since in this study the efficiency definition changes depending on the mode of operation, it is important to see how the overall system efficiency compares between the three control methods. The results reflect the overall slight advantage that the optimization approach offers.

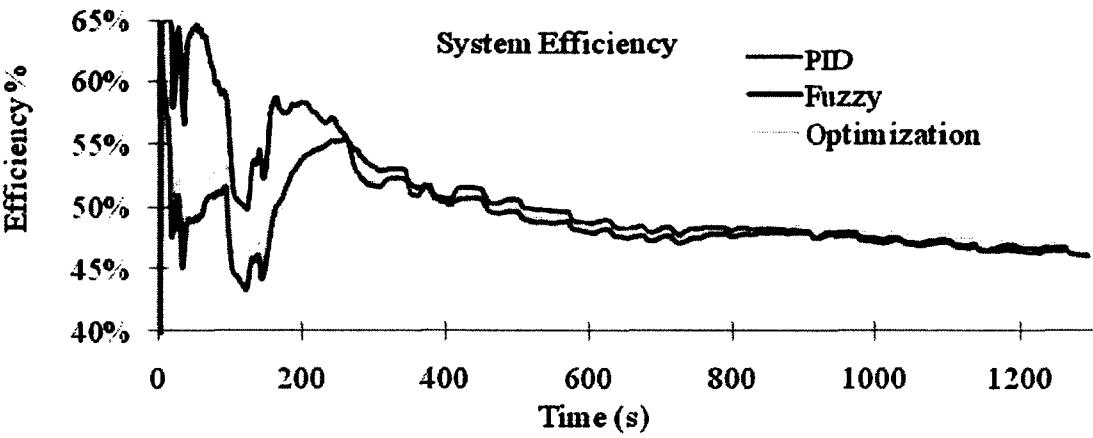


Figure 29: System efficiency

4.4 Partial SOC battery cycling

Figure 30 shows the statistical count of number of charge/discharge cycles the battery goes through when using each control method. As mentioned before, the number of discharge/charge cycles is directly related to the battery life. The goal is to always minimize the number of times the battery goes through a complete charge/discharge cycles. Although the battery is not discharged entirely over a period of 20 minutes, the partial SOC cycling is also critical, and can be used as a performance measure.

Figure 30 also shows the total number cycles from each control method is fairly close; however, the difference is in the magnitude of discharge and charge cycles. In order to quantify the numbers shown, they can be compared to the battery-only electric vehicle case results shown previously in Figure 24. The total number of discharge cycles obtained with hybrid vehicle is around 84 with a PID controller, 86 with a fuzzy logic

controller and 90 with an optimization based controller. The total number of discharge cycles obtained with the battery-only simulation on the other hand is 34 cycles. This comparison already shows the impact of using a hybrid configuration on the battery life, where using the fuel cell to charge the battery results in a significant increase in the partial SOC cycle count.

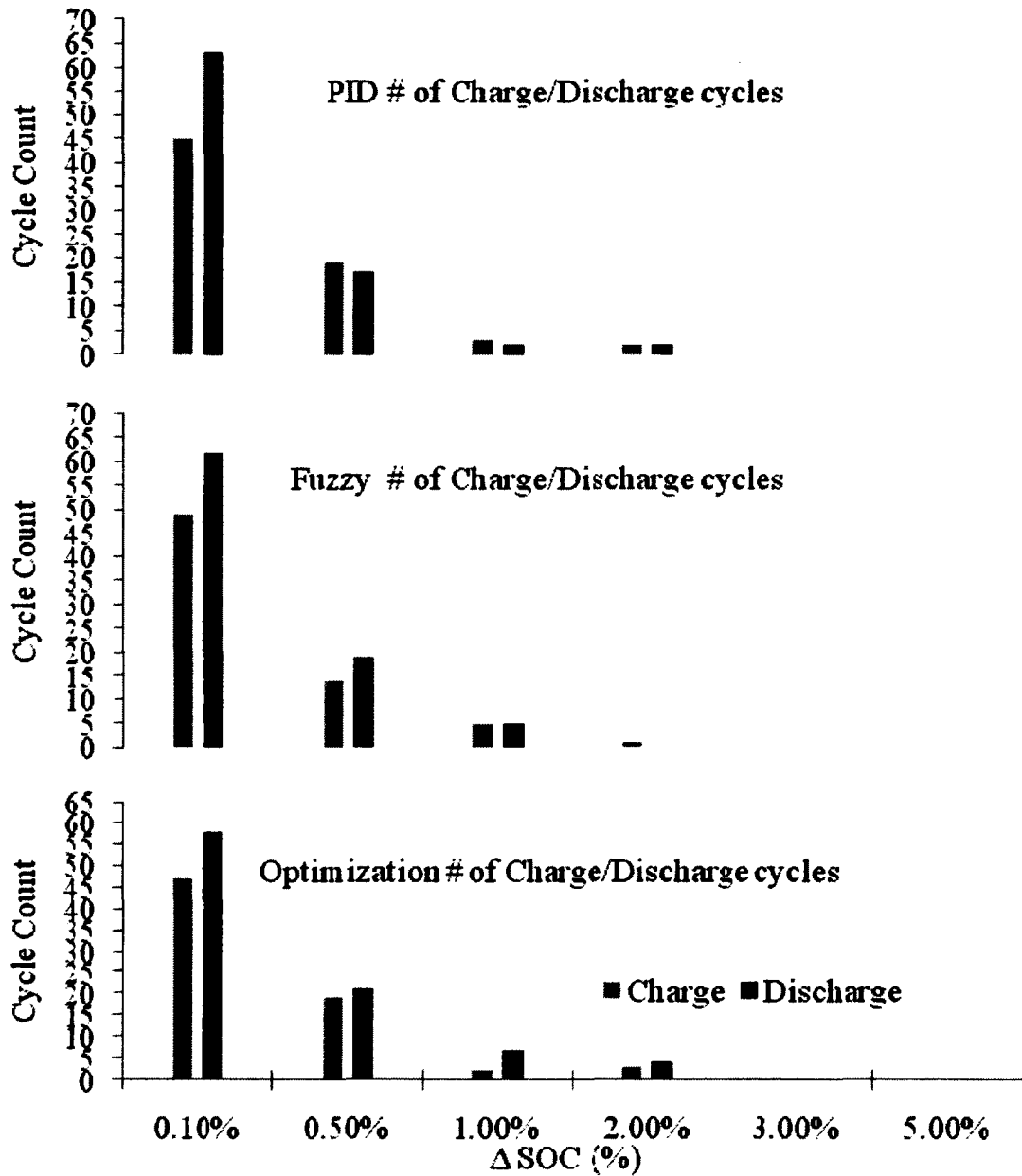


Figure 30: Battery cycle count

Going back to Figure 30, when considering the battery in discharge mode, it is clearly shown that the number of cycles at small magnitudes is very much the same as all three controllers if the discharge magnitude is less than 0.1% change in SOC. However, as the magnitude of the change in SOC increases, the optimization approach seems to have the largest number of discharge cycles. This can be seen at 0.5 %, 1%, and 2% change in SOC magnitudes, where the optimization approach has a total number of cycles of 32 compared with 21 for PID and 24 for fuzzy logic. In the case of charging cycles, the PID control method has the largest number of charging cycles at most magnitudes, with a small of decrease at lower SOC change magnitudes. This can be justified by the fact that the PID controller is more focused on charging the battery to a desired SOC, where the SOC is constantly monitored and maintained at 60%. The optimization approach on the other hand, has the least number of charge cycles when compared with the other two control methods, which is expected given how it optimizes the fuel consumption by limiting the fuel cell contribution. Overall, the optimization approach seems to have the most impact on the battery life by forcing it to go through more discharge cycles. However, determining how much that increase in the number of cycling has on the battery life is a different research area in on its own, and there is no clear way of telling whether a slight increase in the cycle count is as significant as the fuel consumption savings to the designer. A summary of the total number of charge/discharge cycle count is shown in Table 5.

Table 5: Charge/discharge cycle count

	PID		Fuzzy		Optimization	
	Discharge	Charge	Discharge	Charge	Discharge	Charge
0.1%	63	45	62	49	58	47
0.5%	17	19	19	14	21	19
1.0%	2	3	5	5	7	2
2.0%	2	2	0	1	4	3
3.0%	0	0	0	0	0	0
5.0%	0	0	0	0	0	0

CHAPTER V. EXPERIMENTAL

5.1 Experimental Setup

The ultimate goal of this research is to eventually be able to implement a full sized fuel cell vehicle that is capable of performing at the same level as its equivalent size internal combustion engine vehicles with much improved energy efficiency. While MATLAB/Simulink provides an excellent platform to design such a vehicle, the robustness of the design must be validated on the real electric powertrain components. Thus, an experimental test bench is needed to validate the designed power management control methods. The test bench implemented in this research is explained by the schematic in Figure 31.

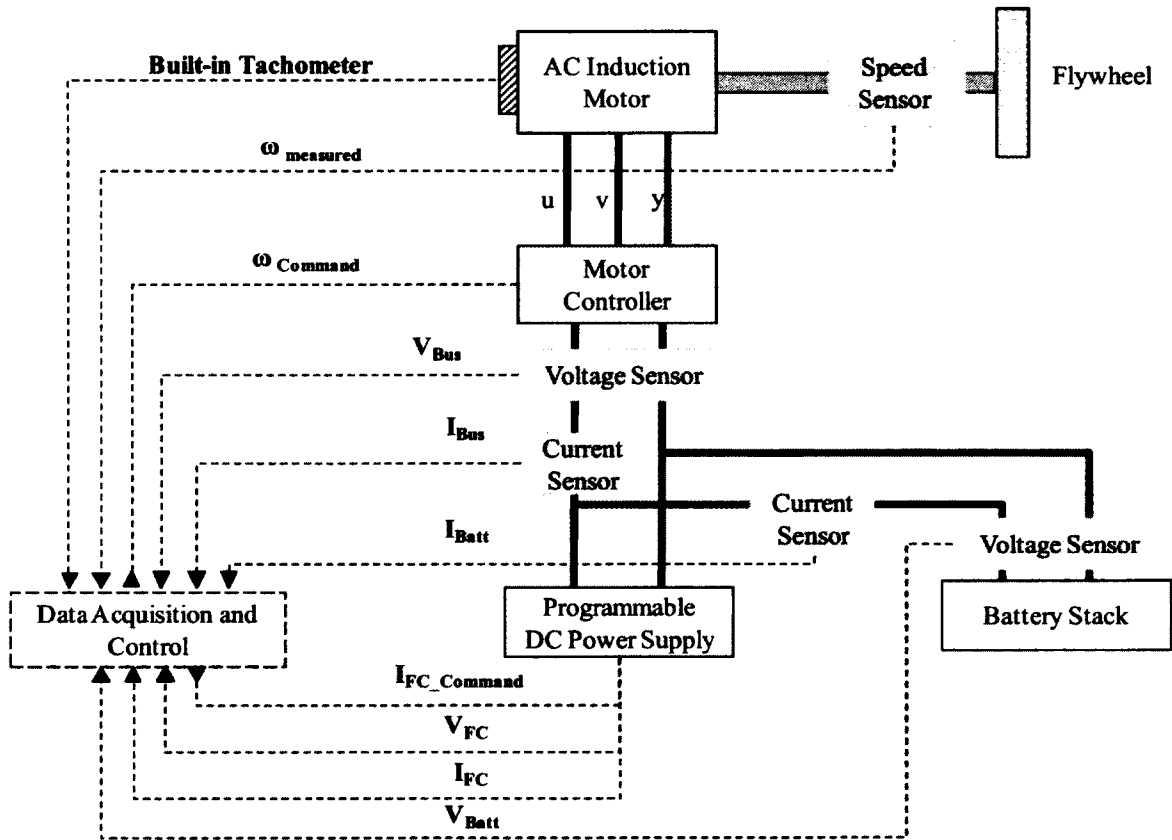


Figure 31: Test bench schematic diagram

The test bench serves as a prototype for the electrical and some of the mechanical components of the fuel cell vehicle powertrain. The test bench is constructed using an “HIL” [34] (Hardware in the Loop) configuration, where parts of the powertrain are

simulated using mathematical models. With HIL, it is possible to implement the designed control algorithms in real time even with only part of the electric powertrain components available. The HIL test bench is implemented using a National Instruments data acquisition card which means that the control algorithms must be transferred from the MATLAB/Simulink environment to the NI Labview environment. This was done by implementing the control algorithms using lookup tables that were constructed by varying the input variables of the fuzzy and the optimization control algorithms. The main sensors used on the test bench are the current, voltage and speed sensors, all of which are Hall Effect sensors. The data is collected in real time and used to determine the hybrid controller output. The rest of the test bench components are broken-down in the next section.

5.1.1 Vehicle Loads

In order to simulate the vehicle powertrain, the road load must be simulated on the electric motor drive, which can be done by coupling the electric motor to a dynamometer. A dynamometer can be defined as “an instrument for measuring energy expended” [35]. There are several types of dynamometers used in experimental test benches. Dynamometers are normally characterized based on their operation range. Some dynamometers can only act as loads on the vehicle drive, while others can simulate loads acting on the vehicle drive as well as regenerative braking. For the purpose of simulating a fuel cell vehicle, it is important that the dynamometer can simulate both driving loads and regenerative braking. The simplest forms of dynamometers are inertia dynamometers. An inertia dynamometer is simply a rotating flywheel that is coupled to the vehicle drive either directly or via a chain or a belt drive. By knowing the geometry and mass of the rotating flywheel, it is possible to calculate the torque required to accelerate the flywheel. Due to its simplicity and ease of instrumentation and control, an inertia dynamometer is selected to be the load for the test bench. This idea was mainly inspired by an existing work done at the University of Waterloo, where a flywheel dynamometer was used to simulate hybrid regenerative braking [36]. The main disadvantage with this type of dynamometer is that it is only capable of simulating acceleration loads, thus, the road slope, wind resistance and rolling resistance of the

vehicle will not be simulated. Nonetheless, this is still a valid simulation of the fuel cell vehicle, mainly because the driving cycle simulates “stop-go” city driving conditions, which is mainly characterized by frequent acceleration and deceleration. Thus, the impact of wind resistance and rolling resistance is not as critical.

As mentioned in the previous sections, the vehicle chosen as the application in this research is the SAE Baja vehicle. Thus, the flywheel design specifications are chosen to simulate the loads the Baja vehicle experiences in acceleration and deceleration. The total kinetic energy the selected flywheel can store is shown in Figure 32.

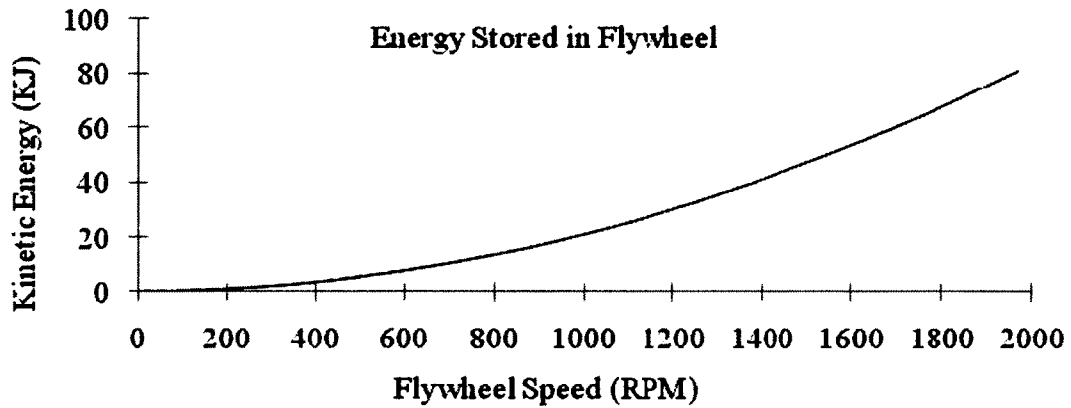


Figure 32: Flywheel kinetic energy

The flywheel dimensions are chosen based on the following equation:

$$I_{flywheel} = \frac{T}{\alpha} = \frac{m_{vehicle}ar}{\alpha} = \frac{m_{vehicle}\alpha r^2}{\alpha} = m_{vehicle}r^2 \quad (46)$$

Where,

$$I_{flywheel} = \frac{1}{2}m_{flywheel}r^2 \quad (47)$$

5.1.2 Electric Motor

There are several options for the electric motor drive, such as an AC Induction, Switched reluctance, DC Brushed and Brushless motors. The main factors that dictate the selection of an electric motor type are: Cost, weight, complexity of control and efficiency. Due to its higher efficiency and relatively lower cost an AC induction motor

was selected to drive the SAE Baja vehicle. Also these days induction motor control has come a long way that it is not very difficult to find a low voltage motor inverter/controller. The motor is sized based on the Baja vehicle loads at different road grades which are shown in Figure 33.

In order to control the AC motor and interface it to the fuel cell and battery DC bus, a vector drive controller/inverter combination that are normally used for electric fork lift utility vehicles are selected. The advantage of the selected motor controller/inverter is that it is capable of operating at a relatively low voltage range, thus allowing the selecting of a smaller battery stack. The motor controller/inverter is rated at 48 Volts and 350 Amps.

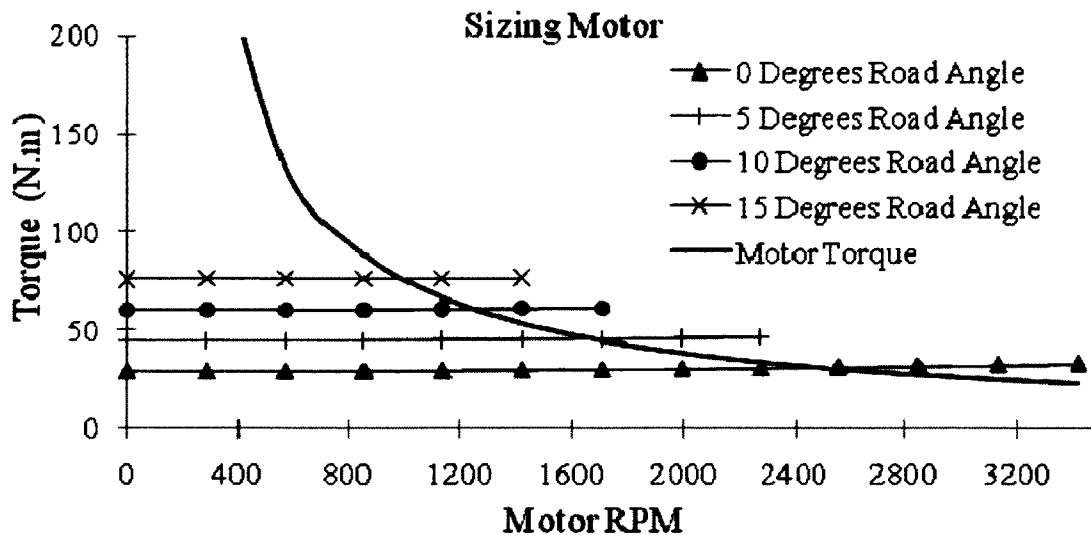


Figure 33: SAE Baja vehicle driving loads

5.1.3 Battery and Fuel Cell

In order to reduce the complexity of the system and also cost of acquiring a fuel cell engine, the fuel cell is simulated using a programmable power supply. The power supply allows its output to vary according to a mathematical model that represents the fuel cell output voltage under different current load conditions. The battery stack on the other hand is constructed from scratch using lithium iron phosphate battery cells that output a nominal individual cell voltage of 3.3 volts. Thus, in order to supply the 48 Volts

required by the electric drive, 15 battery cells are connected in series to give an average of 50 volts and total capacity of 10 Ah.

Despite their significantly higher energy density and light weight, lithium based batteries are very sensitive to being over charged or over discharged. In fact, a lithium iron phosphate battery cell could easily die or lose a significant percentage of its capacity if discharged below 2.1 or charged over 3.6 volts. For that reason, a lithium battery stack must be coupled with a battery management system (BMS) that ensures each battery cell is not over charged / discharged.

5.2 Experimental Results

5.2.1 Model Validation

The main difference between the experimental setup and the mathematical simulations is in the simulated vehicle loads, where in the experimental setup, the flywheel can only simulate acceleration resistance forces acting on the vehicle (i.e at constant speed operation, the electric drive will be under no loads). Thus, with a flywheel type dynamometer, the only method of increasing the load acting on the electric drive is by either increasing the top speed or decreasing the time duration of the driving cycle.

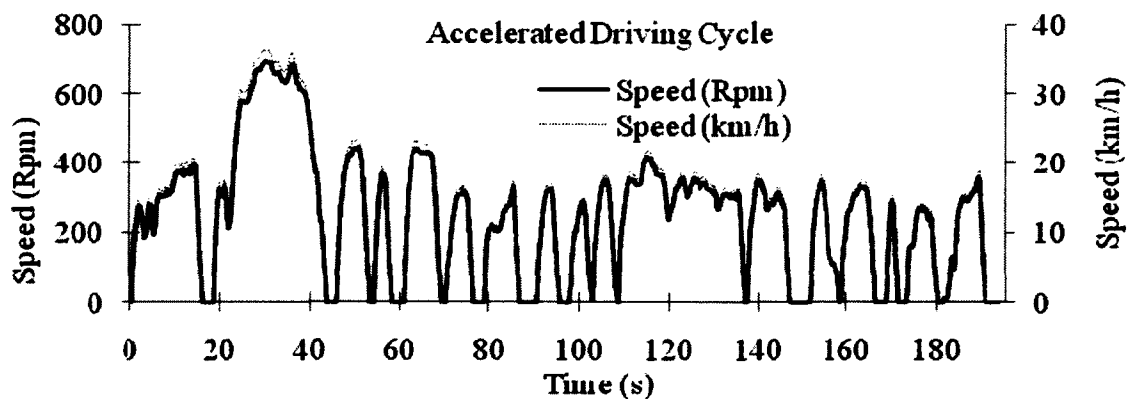


Figure 34: Accelerated driving cycle

The experimental cycle is shown in Figure 34. Given the risks associated with spinning the flywheel dynamometer at high speeds (greater than 1000 rpm), the driving

cycle duration is decreased instead resulting in an experimental driving cycle input that takes only 200 seconds (3.33 minutes) to run.

In order to quantify how the experimental setup matches the desired simulation, the mathematical model in MATLAB/Simulink was modified by adjusting the driving cycle to the accelerated cycle. Also, the longitudinal vehicle dynamics model was modified to only take into consideration the inertial forces acting on the vehicle. A direct comparison of the electrical power demanded by the load in the experimental setup and the mathematical simulation model is shown in Figure 35, where both the simulation and experimental power demands are calculated based on the electrical measurements of the system (i.e. power = Total current x Bus Voltage).

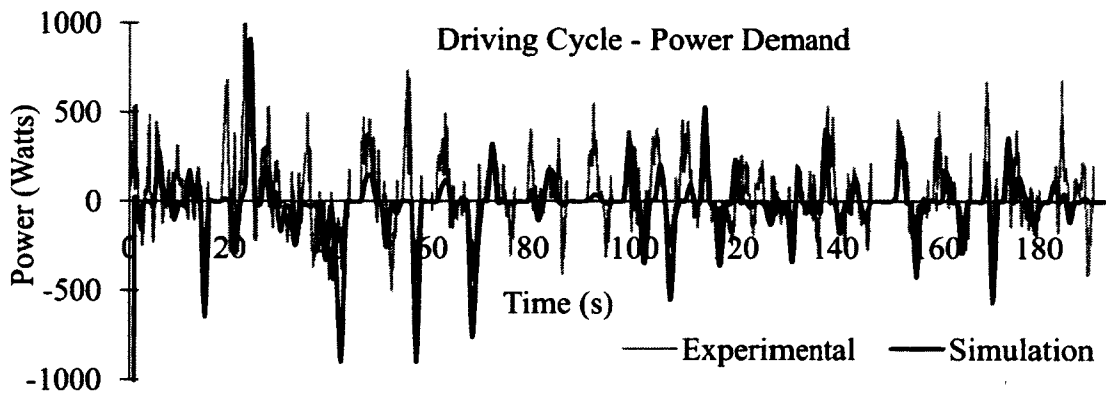


Figure 35: Total power demand comparison

From the comparison, the experimental power demand seems to follow the general acceleration and regenerative braking patterns of the expected power demand in the simulation, however, there are several points on the curve where the experimental power demand significantly overshoots the targeted simulation power demand in acceleration mode or undershoot the simulation in regenerative braking. These discrepancies can be explained by three main factors that are not considered in the simulation model. The first obvious reason is the accuracy of the mathematical model used in the simulation. As mentioned in the previous sections the model for the electric motor drive is constructed using an efficiency lookup table, thus, it does not take into consideration time delays, controller tuning or efficiency losses in the system due to AC

to DC power conversions. The second factor is due to the fact that the speed of the motor in the experimental setup is controlled using PID controller that adjusts the command to the motor controller based on the measured speed of the motor. Thus, any overshoot in the PID controller output will result in an overshoot in the motor response and thus, the DC bus will experience a spike in the current demand. The third factor that the simulated loads do not match the experimental loads can be attributed to the braking method used to slow down the electric motor. In this experimental setup, the AC motor drive is configured to use electromagnetic braking to slow down the motor shaft, which means the motor drive would become an Eddy Current brake reversing the electromagnetic field to act against the load torque and thus slowing it down. Thus, as the motor is commanded to slow down, the DC bus experiences a quick and sharp spike in the supplied power.

A second comparison was done between the measured output speed at the motor shaft and the output speed in the simulation model. The comparison is shown in Figure 36. In general the magnitude of the measured speed matches the simulation speed when the vehicle is in acceleration. However, in deceleration, the motor shaft speed does not match the simulation speed and thus results in a less amount of regenerative braking power sent back to the battery stack. This can also be seen in the experimental power curve shown in Figure 35, where the magnitude of negative power in the experimental results is noticeably less than the simulation results.

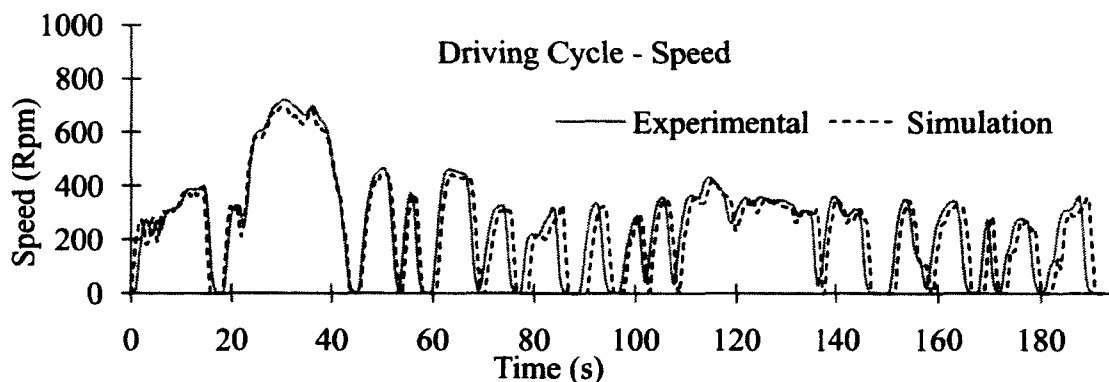


Figure 36: Speed comparison

5.2.2 Controller Output Validation

The main objective of the experimental setup is to be able to validate if the comparison results between the three control methods obtained in the mathematical model do in fact remain true for the real system. As shown earlier the power demand obtained using the experimental setup does not exactly match the mathematically simulated power demand, thus, a direct quantitative comparison is not very indicative of whether or not the experimental results match the simulation results. Instead, the results are compared by considering the patterns of how the outputs of controllers behave with respect to each other.

In the case of the battery SOC variation during the accelerated driving cycle, the results are shown in Figure 37. Although, the battery SOC does not vary significantly (less than 1% change), the pattern in the SOC variation using each control method is indicative of whether or not the controller is operating as expected from the simulation model. Once again the difference between the three control methods is how aggressive they are in maintaining the SOC of the battery, from Figure 37 it is clear to see that the PID control method is the most aggressive in maintaining the SOC of the battery and hence, the SOC stays the closest to 60%, while using the other two controllers we can see that the battery is allowed to discharge deeper.

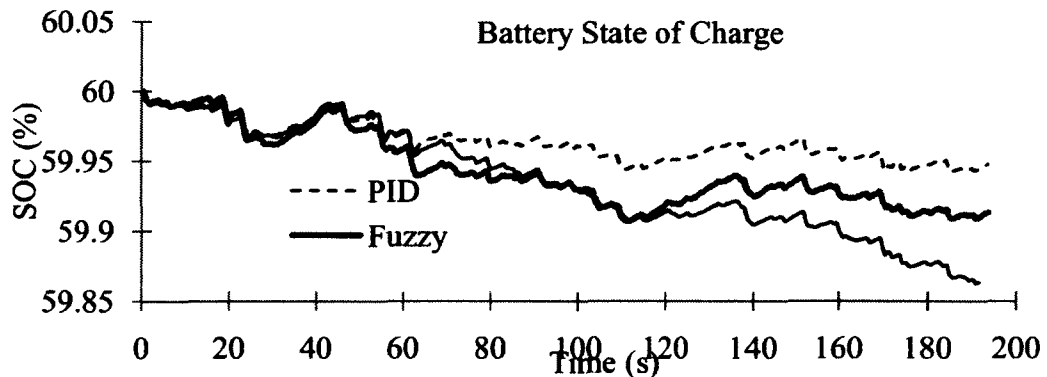


Figure 37: Experimental SOC variation

The battery SOC data collected from the experiment in general seem to support the simulation results and can be summarized as follows:

- The PID controller forces the battery to contribute to help the fuel cell only when the vehicle is under high transient power demands that the fuel cell is not capable of providing. Thus, the PID control method in the experimental setup works as a load leveling power management strategy.
- The fuzzy logic controller operates in different modes depending the SOC of the battery and the total power demand, thus, allowing the battery to make a slight contribution to the overall power demand, while also buffering the transient power demands from the fuel cell.
- The optimization controller is the most reliant on the power from the battery, and thus the deepest SOC change is seen in the results graph. Essentially, this controller finds the most optimum power split between the fuel cell and the battery, without worrying about deep cycle discharges in the battery.

The total fuel consumption using each control method is considered next. The results are shown in Figure 38.

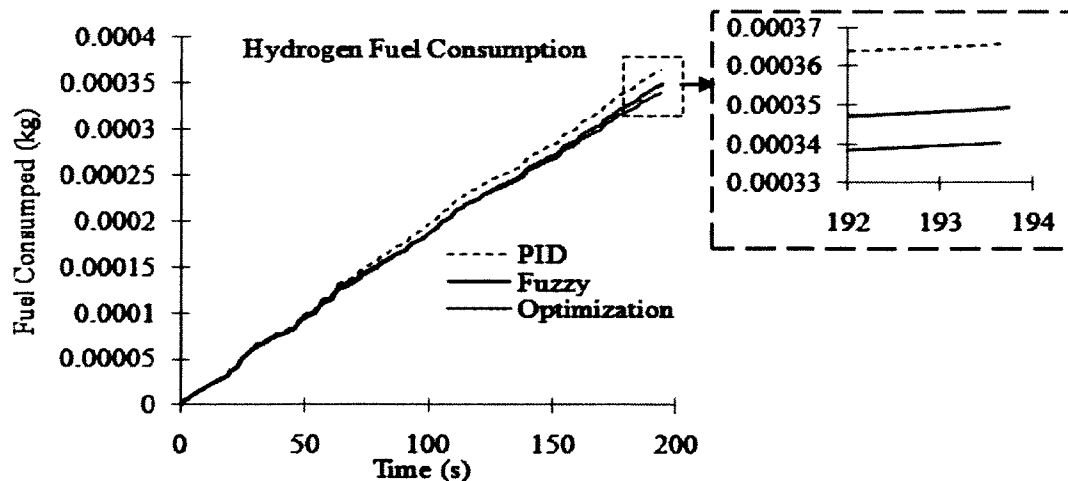


Figure 38: Experimental fuel consumption

The results show that the optimization approach has the least fuel consumption over the driving cycle, which coincides with the mathematical simulations. However, the amount of fuel saved is on the order of 0.0000111 kg, which corresponds to a hydrogen

fuel tank of 0.02417 liter. Thus, the difference between using the fuzzy logic or the optimization approach would be a hydrogen fuel tank volume savings of 0.00079 liter, which is very insignificant even when considering a longer traveling distance. Table 6 shows a summary of the results.

Table 6: Summary of experimental fuel consumption results

	Distance Traveled	Total Fuel Consumed	H2 Density @ 35 MPA (kg H2 / L)	Gas Tank Volume (L)
PID Method	8 km	0.0003656	0.014	0.02611
fuzzy Method	8 km	0.0003495	0.014	0.02496
Optimization Method	8 km	0.0003	0.014	0.02417

The last comparison criteria between the control methods is their impact on the battery health, which is indicated by the number of charge/discharge cycles the battery has to go through during the driving cycle. Figure 39 shows the total number of charge/discharge cycles from the experimental results. Since the total change in the SOC is very small, only the total number of cycles is considered, meaning that each change in the sign of the SOC is counted as a beginning of a charge or discharge cycle, regardless of the magnitude. The PID control method results in the largest number of cycles in the battery, which can be explained by the goal of this method which is to keep the SOC near 60% at all times. The fuzzy and the optimization approaches result in a very close number of charge/discharge cycles. Therefore, even if the magnitude is small, the results obtained from the experiment are very similar to the simulation results if the small cycle count is considered from Figure 30.

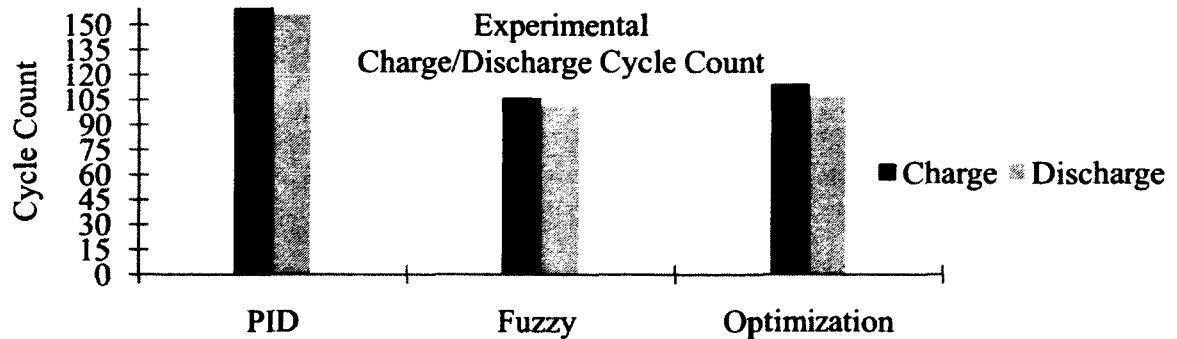


Figure 39: Experimental battery cycle count

Chapter VI. Conclusions and Recommendations

6.1 Conclusions

Considering the direct comparison results presented in the previous chapter, it is difficult to make a conclusion on which control methodology is the most appropriate for this application, since that really depends on the priorities of the designer. The results have clearly shown that the instantaneous optimization results in the least fuel consumption and thus most efficient hybrid configuration. However, the results also show that savings in the fuel consumption are small when compared to fuel consumption numbers of similar cars that are currently on the road. The other main factor that was considered in the comparison is the battery cycling using each control method. In general it was shown using both the simulation and experimentally, that the optimization approach results in the least number of cycles if the cycle magnitude is very small (on the order of 0.1 % SOC) however, when looking at cycles with larger magnitudes, the optimization approach forces the battery through the most charge/discharge cycles. Thus, there seems to be a tradeoff between improving the fuel consumption of the vehicle or improving the degradation time of its powertrain components. Deciding which factor is more important will depend on the application. Also it should be mentioned that although it is true that partial SOC cycling can result in battery capacity degradation, there is still no clear indication of how much the partial SOC cycling the battery can withstand before it starts to degrade. Overall, the comparison between the three control methods is shown in Table 7.

Table 7: Summary of comparison

	PID	Fuzzy Logic	Optimization
Strategy	Load leveling	Rule based	Load following
Fuel Efficiency	Lowest	In the middle	Highest
Battery Cycling	Small cycles	Small cycles	Big cycles

To summarize, the main accomplishment of this work is in presenting an alternative local optimization approach that does not require prior knowledge of the driving cycle and a set of performance measures to evaluate the effectiveness of the proposed approach. In order to validate the effectiveness of the optimization approach,

standard performance measures that consider battery life, fuel consumption and system efficiency were developed. In addition to that, the experimental setup used to validate the simulation results presents a platform for further work that can be done in the area of power management and electric vehicle powertrain design.

6.2 Recommendations

The recommendations are divided into two parts: future work on power management strategy and improvements on the experimental setup.

6.2.1 Future Work on Power Management Strategies

Perhaps one of the most useful conclusions taken from this research work is pertaining to the impact of power management control methods on the life cycle of the battery stack. While the method used to evaluate the battery health (cycle counting) represents a good indicator of the degradation in the battery capacity, it is not an accurate way to evaluate the state of health of the battery stack. Thus, there is a need for an accurate way to evaluate the battery health with minimal reliance on experimental data. Another improvement area in the presented power management evaluation method is in evaluating the fuel cell degradation. This work does not take into consideration the life cycle of the fuel cell system, since constraints are already imposed on the rate and top limit of the fuel cell output. However, the power management strategy could have an impact on both the fuel cell and the battery stack, thus there needs to be a method to evaluate the degradation in the fuel cell capacity.

6.2.2 Improvements on the Experimental Setup

While using a flywheel to serve as an inertia dynamometer for experimental validation is a quick and less expensive method, it has its drawbacks. One of the main disadvantages of the experimental setup used in this research is its inability to apply loads on the motor while rotating at constant speed. For that reason, the test bench could be improved with one of the two following options:

Option #1 Expand on the existing inertia dynamometer: The existing inertial dynamometer that was built has its own drawbacks such as lack of control over load applied and inability to simulate loads at constant speeds. However, these problems can be fixed by adding an electric eddy brake dynamometer to the existing setup. With this option, the ability of the inertia dynamometer to simulate regenerative braking along with the ability of the electric eddy brake to generate loads at constant speeds can be combined to form a complete four quadrant dynamometer test bench setup. The proposed idea is depicted in the following schematic in Figure 40. The main advantage of this setup is lower cost associated with inertial and eddy current brake dynamometers.

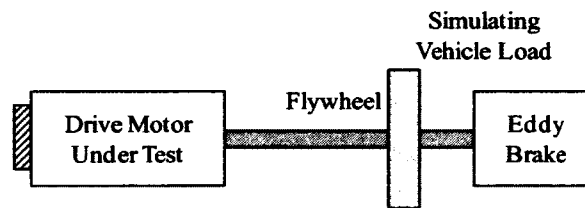


Figure 40: Option #1 for improving the test bench

Option #2 Use an electric motor dynamometer: While the combination of an eddy current brake and inertia dynamometers presents an ideal economical option, it is still not as flexible as using an electric motor to apply loads on the motor under test. From a safety point of view having a big flywheel rotating at high speed might not be feasible for simulating driving conditions with high regenerative braking energy. Thus, using a flywheel-electric brake combination will limit the range of vehicles that can be simulated on the test bench. An electric motor dynamometer on the other hand can accommodate a wide range of vehicle sizes given the appropriate control methods. The proposed schematic is shown in Figure 41:

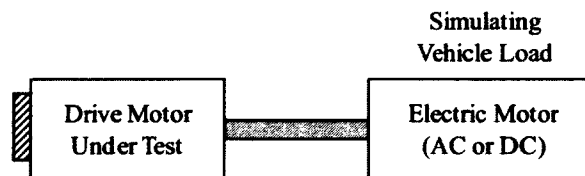


Figure 41: Option #2 for improving the test bench

Either an AC or a DC motor can be used for the dynamometer, the selection will most likely depend on the efficiency and ease of control of the dynamometer and also cost.

References

- [1] "Fuel cell light duty vehicles". <http://www.fuelcells.org/info/charts.html>. Accessed on September, 2009.
- [2] "First FCX clarity". World.Honda.com. Honda. <http://world.honda.com/news/2008/4080616First-FCX-Clarity>. Accessed on January, 2010.
- [3] C.E Thomas. "Fuel cell battery electric vehicles compared". International Journal of Hydrogen Energy. 34 (2009): 6005-6020.
- [4] M. Kromer and J. Heywood. "Electric power trains: opportunities and challenges in the US light-duty vehicle fleet". Sloan Automotive Laboratory: Massachusetts Institute of Technology. 2007: LFEE 2007-03 RP.
- [5] B. D. McNicola, D. Rand, and R. Williams. "Fuel cells for road transportation purposes — yes or no?". Journal of Power Sources. 100 (2001): 47–59.
- [6] Junhyun Choa, Han-Sang, Kima, and Kyoungdoug Min. "Transient response of a unit proton-exchange membrane fuel cell under various operating conditions". Journal of Power Sources. 185 (2008): 118-128.
- [7] Rod Borupa, Daveya John, Fernando Garzona, David Wood, and Michael Inbody. "PEM fuel cell electrocatalyst durability measurements". Journal of Power Sources. 163 (2007): 76-81.
- [8] Stefan Pischingera, Carsten Schönfeldera, and Jürgen Ogrzewallab. "Analysis of dynamic requirements for fuel cell systems for vehicle applications". Journal of Power Sources 154 (2006): 420-427.
- [9] Walter van Schalkwijk and Bruno Scrosati. "Advances in Lithium-ion battery technologies". Kluwer Academic Publishers. 2002.
- [10] Zhenhua Jiang, Lijun Gao, Mark Blackwelder and Roger Dougal. "Design and experimental tests of control strategies for active hybrid fuel cell/battery power sources". Journal of Power Sources. 130 (2004) 163-171.
- [11] Phatiphat Thounthong, Stephane Rael and Bernard Davat. "Control strategy of fuel cell/supercapacitors hybrid power sources for electric vehicle". Journal of Power Sources. 158 (2006) 806-814.

- [12] Lino Guzzella and Antonio Sciarretta. "Vehicle Propulsion Systems". Springer-Verlag Berlin Heidelberg. 2005.
- [13] Kwi-Seong Jeong, Won-Yong Lee and Chang-Soo Kim. "Energy management strategies of a fuel cell/battery hybrid system using fuzzy logics". *Journal of Power Sources*. 145 (2005) 319-326.
- [14] M.C. Kisacikoglua, M. Uzunoglua and M.S. Alama. "Load sharing using fuzzy logic control in a fuel cell/ultracapacitor hybrid vehicle". *International Journal of Hydrogen Energy*. 34 (2009) 1497-1507.
- [15] Dawei Gao, Zhenhua Jin and Qingchun Lu. "Energy management strategy based on fuzzy logic for a fuel cell hybrid bus". *Journal of Power Sources*. 185 (2008) 311-317.
- [16] Yoon Hyoung-Jin and Lee Se-Jin. "An optimized control strategy for parallel hybrid electric vehicle". *SAE Journal*. 112 (2003) 579-586.
- [17] Wang Shuaiyu, Huang Kaisheng, Jin Zhenhua and Peng Yuanyuan. "Parameter Optimization of Control Strategy for Parallel Hybrid Electric Vehicle". *IEEE Conference on Industrial Electronics and Applications*. (2007) 2010-2012.
- [18] Pierluigi Pisu and Giorgio Rizzoni. "A supervisory Control Strategy for Series Hybrid Electric Vehicles with Two Energy Storage Systems". *Vehicle Power and Propulsion, 2005 IEEE Conference*. (2005): 65-72.
- [19] Lorenzo Serrao. "A comparative analysis of energy management strategies for hybrid electric vehicles". PhD Thesis, Ohio State University. 2009.
- [20] Chun-Yan Li and Guo-Ping Liu. "Optimal fuzzy power control and management of fuel cell/battery hybrid vehicles". *Journal of Power Sources* 192 (2009) 525–533.
- [21] Wenzhong Gao and Chris Mi. "Hybrid vehicle design using global optimization algorithms". *International Journal of Electric and Hybrid Vehicles*. 1 (2007): 57-70.
- [22] Eva Ericsson, Hanna Larsson and Karin Brundell-Frej. "Optimizing route choice for lowest fuel consumption – Potential effects of a new driver support tool". *Transportation Research Part C: Emerging Technologies* 14 (2006): 369-383.

- [23] Marla Barnett, William Bombardier, Micheal Bowie, Marry Burford, Dana Chesnik, X. Ding, Colin Drummond, Ahmad Fadel, Ian Funkenhauser, Herman Hiebert, H. Huang, Carl Jankowski, John Juba, Chris Kelly, Joe Krzemien, Kamil Kubacki, Dylan Langlois, Stephanie Masse, Wade O'Moore, David Pedro and Micheal Smith. "University of Windsor SAE Baja Design". University of Windsor. 2007.
- [24] "Horizon fuel cell technologies". <http://www.horizonfuelcell.com/store/h5000>. Accessed on January, 2009.
- [25] James Larminie and Andrew Dicks. "Fuel cell systems explained". 2nd Edition. West Sussex: John Wiley & Sons Ltd. 2003.
- [26] Colleen Spiegel. Modeling Simulation Using MATLAB. 1st Edition. Elsevier Inc. 2008.
- [27] Siddique Khateeb, Mohammed Farid, Selman Robert, and Said Al-Hallaj. "Mechanical–electrochemical modeling of Li-ion battery designed for an electric scooter". Journal of Power Sources 158 (2006) 673-678.
- [28] Sandeep Dhameja. "Electric vehicle battery systems". Butterworth–Heinemann. 2002.
- [29] Jixin Chen and Biao Zhou. "Diagnosis of PEM fuel cell stacks dynamic behaviors". Journal of Power Sources. 177 (2008) 83-95.
- [30] Ken Kato, Akira Negishi, Ken Nozaki, Izumi Tsuda and Kiyonami Takano. "PSOC cycle testing method for lithium-ion secondary battery". Journal of Power Sources 117 (2003) 118-123.
- [31] Miguel Valdez, Jaime Valera and Ma Arteaga. "Estimating SOC in lead-acid batteries using neural networks in a microcontroller-based charge controller". 2006 International Joint Conference on Neural Networks. (2006) 2713-2719.
- [32] S. Drouilhet and B.L Johnson. "A battery life prediction method for hybrid power applications". National Renewable Energy Laboratory, (1997) 1 - 16.
- [33] "EPA federal test procedures revisions". <http://www.epa.gov/otaq/sftp.htm>. Accessed on January, 2010.

- [34] "Applying an HIL simulation platform for energy systems in hybrid electric vehicles". <http://sine.ni.com/cs/app/doc/p/id/cs-11551>. Accessed on September, 2008.
- [35] A.J Martyr and M.A Plint. "Engine testing". 3rd Edition. New York: Elsevier. 2007.
- [36] Michael Kiers. "Automotive regenerative braking utilizing electrochemical capacitor energy storage". Master's Thesis. University of Waterloo. 2004.

VITA AUCTORIS

NAME: Ahmad Fadel

PLACE OF BIRTH: Al-Başrah, Iraq

YEAR OF BIRTH: 1985

EDUCATION: Henry Street High School, Whitby, Ontario, Canada
2001 – 2003

University of Windsor, Windsor, Ontario, Canada
2003 – 2007 BAsC

University of Windsor, Windsor, Ontario, Canada
2008 – 2010 MASc